ICCM 2020, 2020/06/18

Fast Magnetic Resonance Imaging: Theory, Technique and Application

Dong Liang, PhD

Medical AI Research Center/
Paul C. Lauterbur Research Center for Biomedical Imaging
Shenzhen Institutes of Advanced Technology (SIAT)，CAS

中国科学院深圳先进技术研究院
Shenzhen Institutes of Advanced Technology,Chinese Academy of Sciences

Outline

- Background
- Parallel Imaging
- Compressed sensing based methods
- Deep Learning based methods

Magnetic Resonance Imaging (MRI)

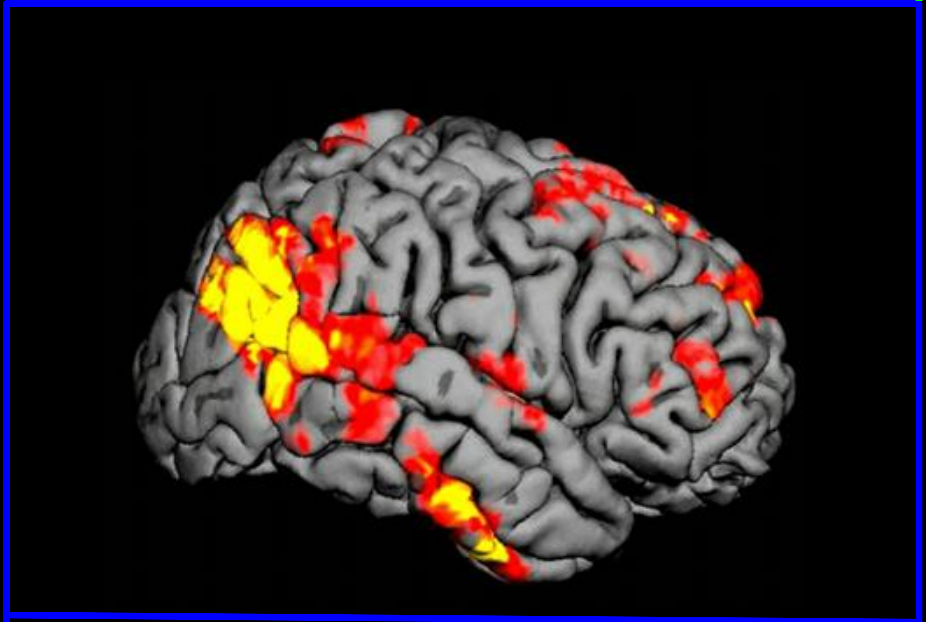

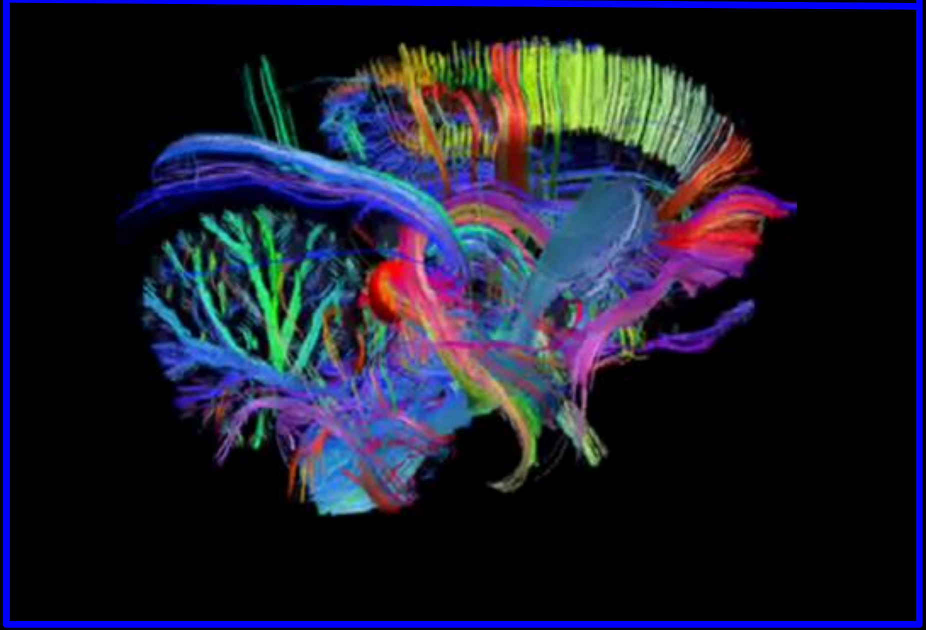

Slow imaging speed is the bottle neck of MRI

Coronary
Artery
Imaging

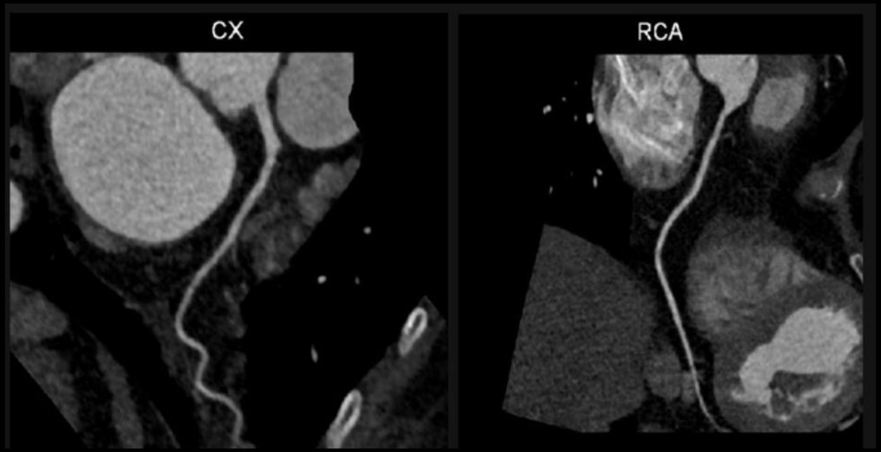

> 15 min

< 1 s

Drawbacks of Long Acquisition Time

Claustrophobia

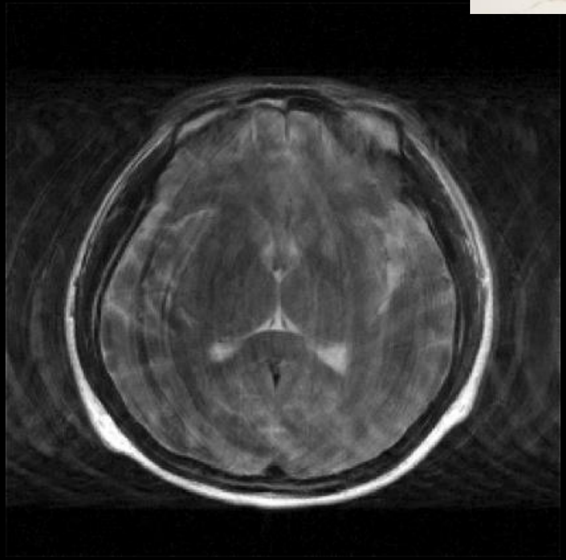

Motion artifacts

High cost

Spatial domain and MR data space

Ideally , the relationship between MR image and k-space data can be formulated as Fourier transform

$$d(\vec{k}) = \int M(\vec{r})\, e^{-j2\pi\vec{k}\vec{r}} \mathrm{d}\vec{r}$$

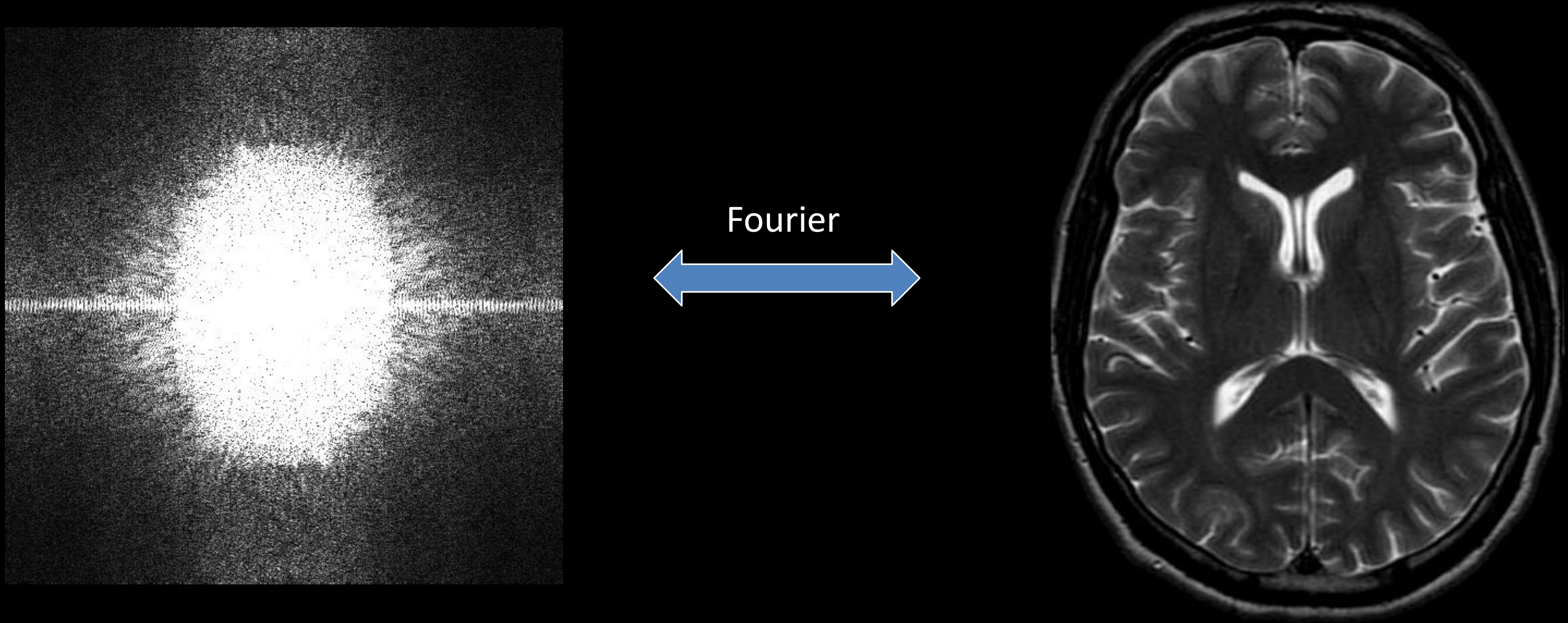

K-space Sampling

Raw data is sampled
in k-space

replications
in image space

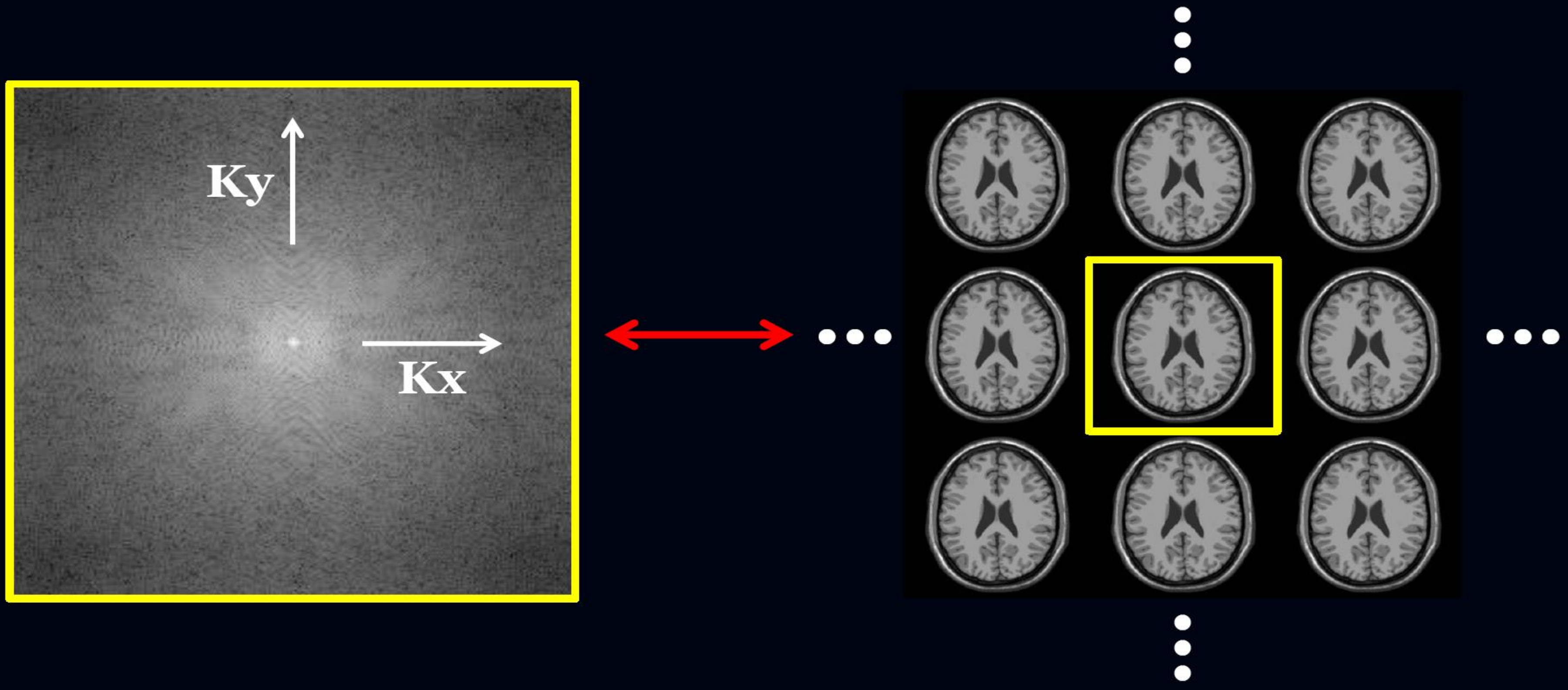

Nyquist-Shannon Sampling Theorem in k-space

NS-sampling

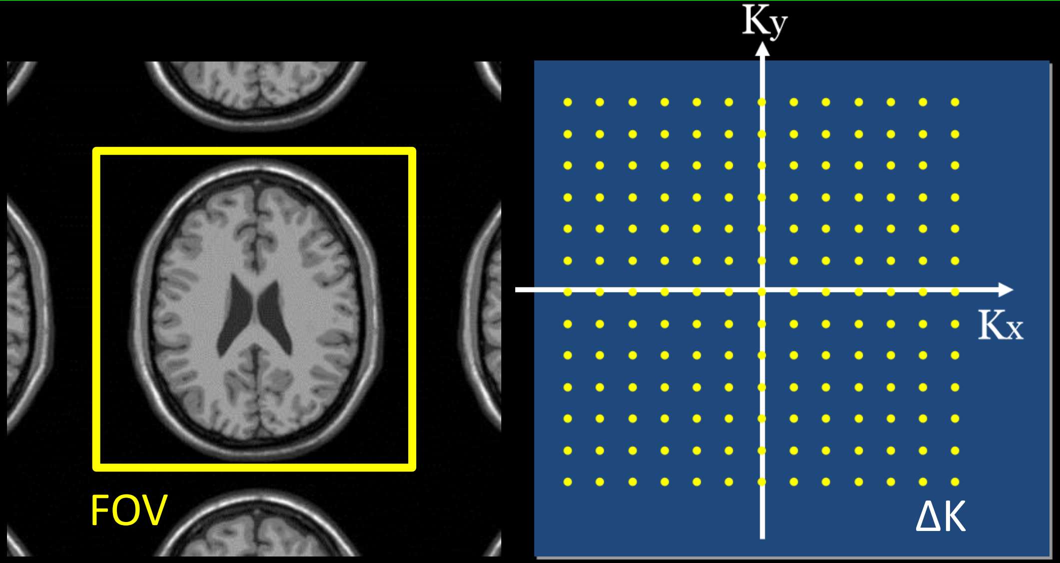

smaller ΔK
larger FOV

Insufficient sampling

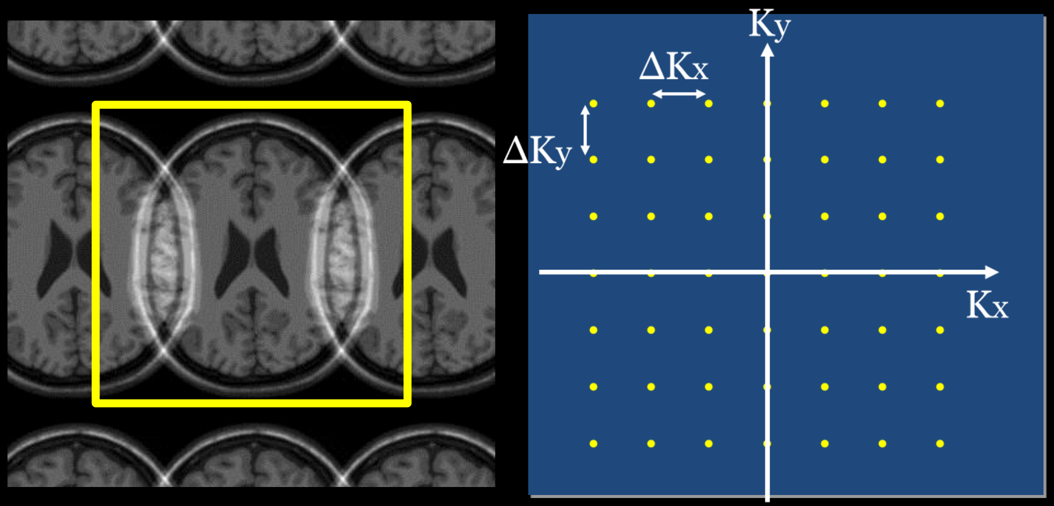

larger ΔK
Smaller FOV

FOV=1/ΔK

The factors that determine the time of acquisition

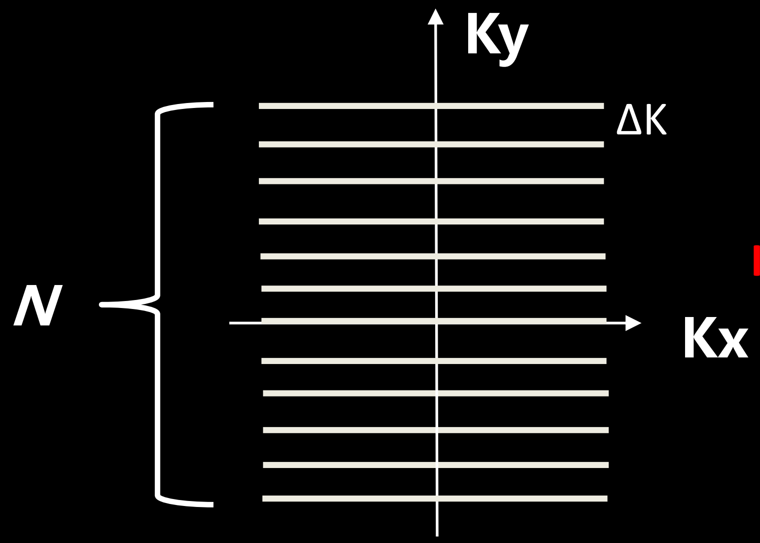

K-space

Inverse Fourier transform

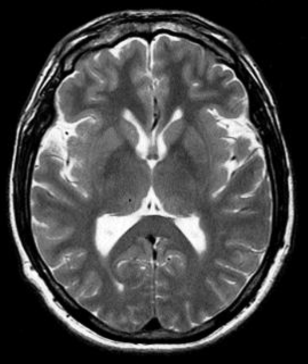

image

$$T = N \downarrow \times TR$$

scan time | collected lines | line time

undersampling

Example: spin echo

T1-weighted (T1w)：TR=800ms， N=256 , T=3.4min

T2-weighted (T2w)：TR=2000ms, N=256, T=8.5min

Accelerate MR imaging from under-sampled k-space

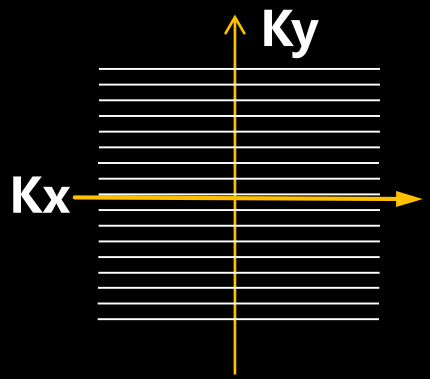

full-sampled
k-space

Nyquist-Shannon sampling theorem

Fourier transform（FT） √ ✕

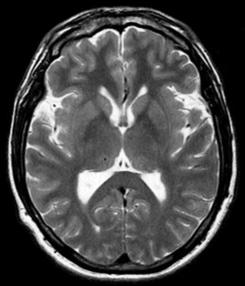

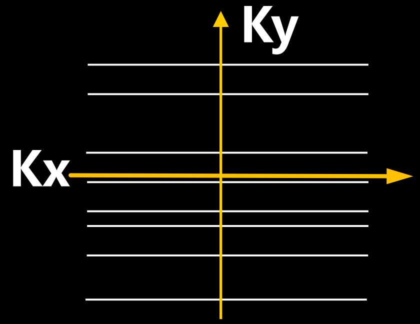

under-sampled
k-space

Image reconstruction

Inverse Problem

Accelerate MR imaging from under-sampled k-space

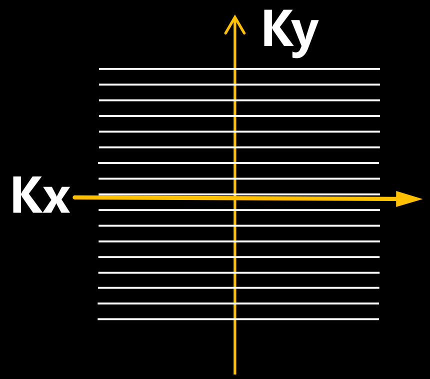

full-sampled k-space

Nyquist-Shannon sampling theorem

Fourier transform（FT） √

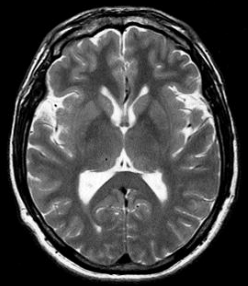

reconstruction

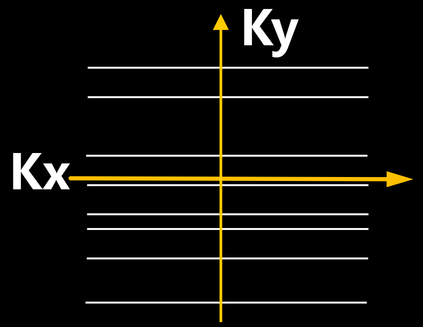

under-sampled k-space

➕

prior information

Some knowledge that were known before scan

Fast magnetic resonance imaging based on prior knowledge

1980s

Partial Fourier
(Conjugate symmetry)

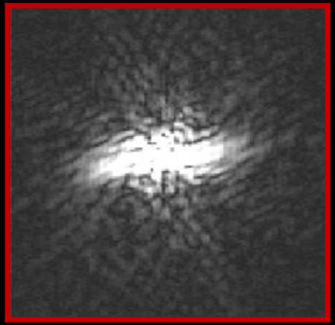

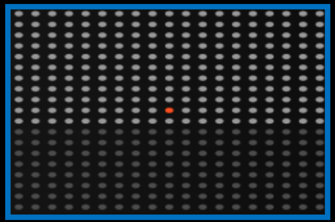

Fourier transform
(1807)

2000s

Parallel imaging
(Coil sensitivity)

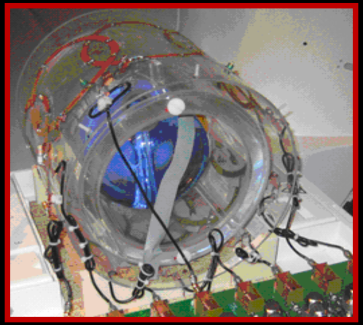

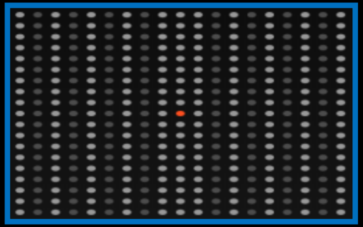

Multi-channel
Sampling theorem
(1976)

2007

Compressed sensing
(Sparse prior)

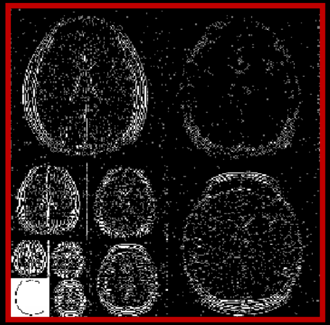

Compressed sensing
(2006)

2016

Artificial intelligence
(big-data prior)

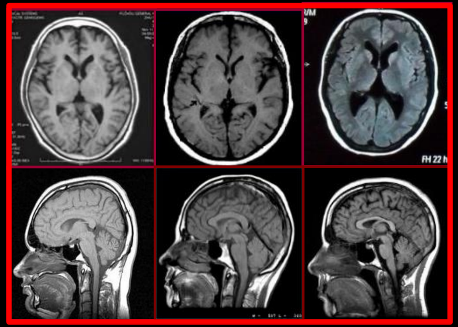

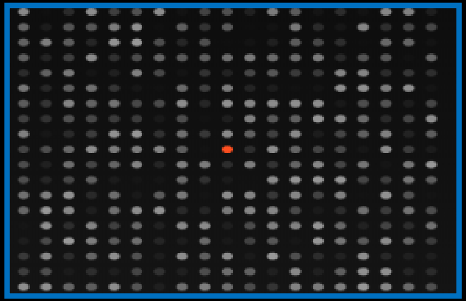

Deep learning
(2006)

The formulation of parallel MR imaging

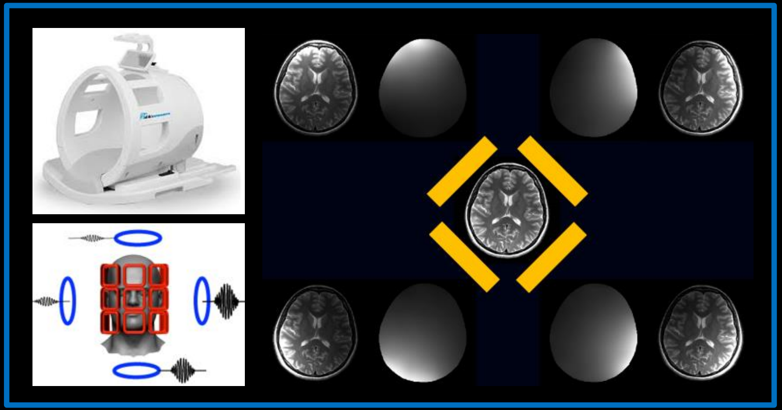

$$s_i(k_x, k_y) = F C_i m(x, y)$$

Sensitivity Encoding

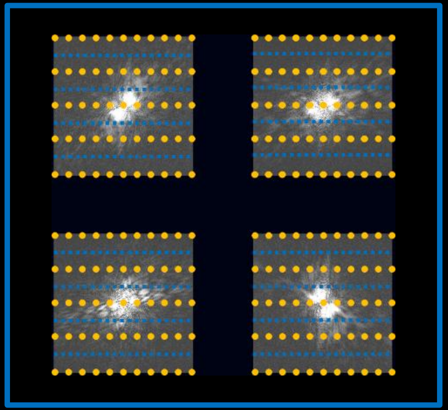

Inverse FFT

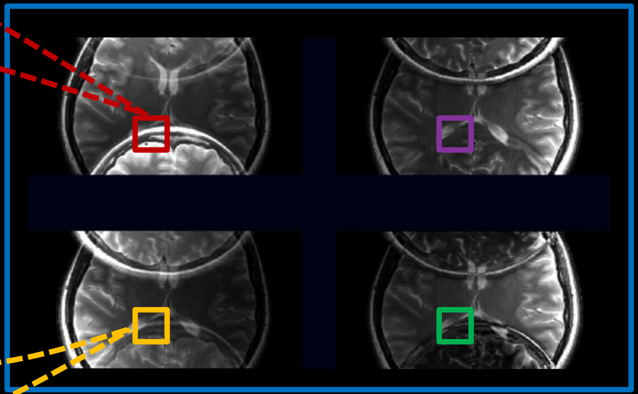

reconstruction

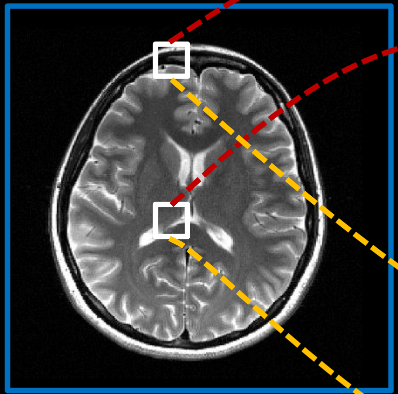

C_{11}

C_{12}

C_{21}

C_{22}

$$\begin{bmatrix} m_{a1} \\ m_{a1} \\ m_{a1} \\ m_{a4} \end{bmatrix} = \begin{bmatrix} C_{11} & C_{12} \\ C_{21} & C_{22} \\ C_{31} & C_{32} \\ C_{41} & C_{42} \end{bmatrix} \begin{bmatrix} m_1 \\ m_2 \end{bmatrix}$$

reconstruction： solve an inverse problem

Condition number： SNR

The problem of parallel MR imaging —low SNR

phenomenon

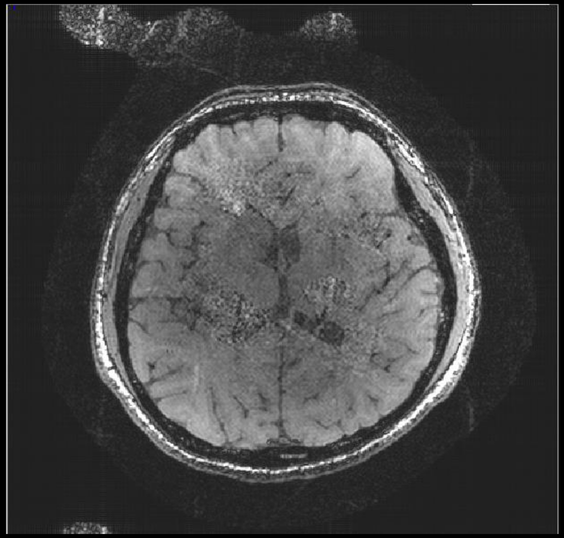

4-fold

Spatially variant noise amplification

Reason

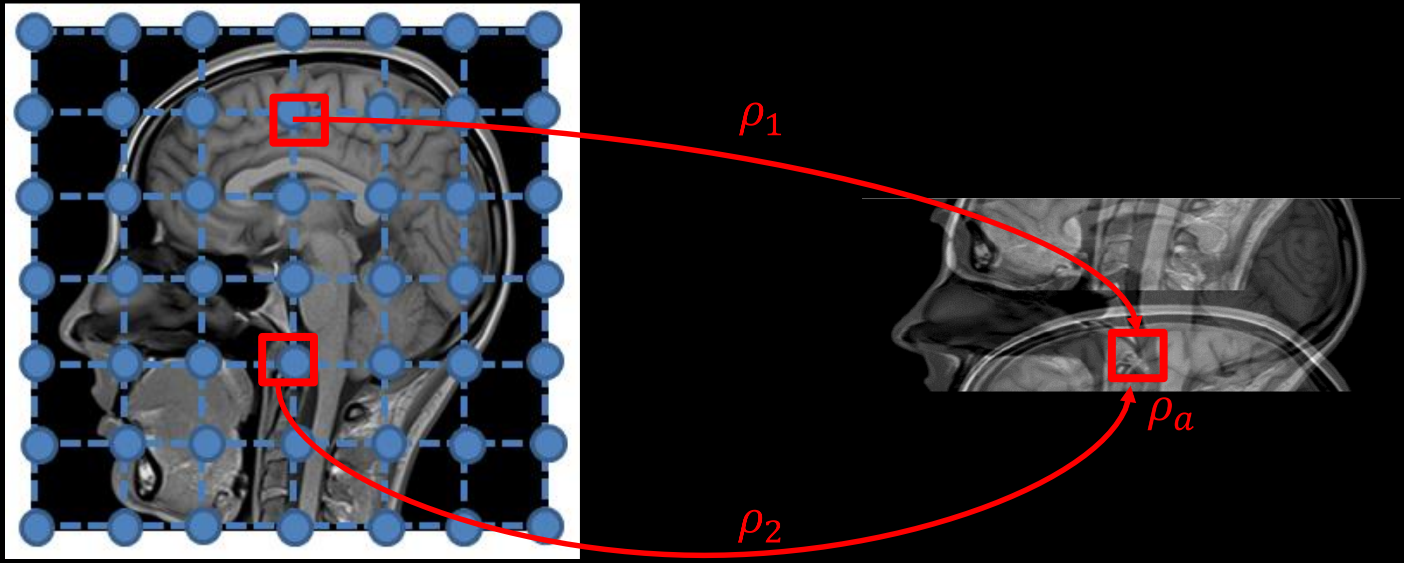

Highly ill-posed

Increasing #equations by using Virtual Coil

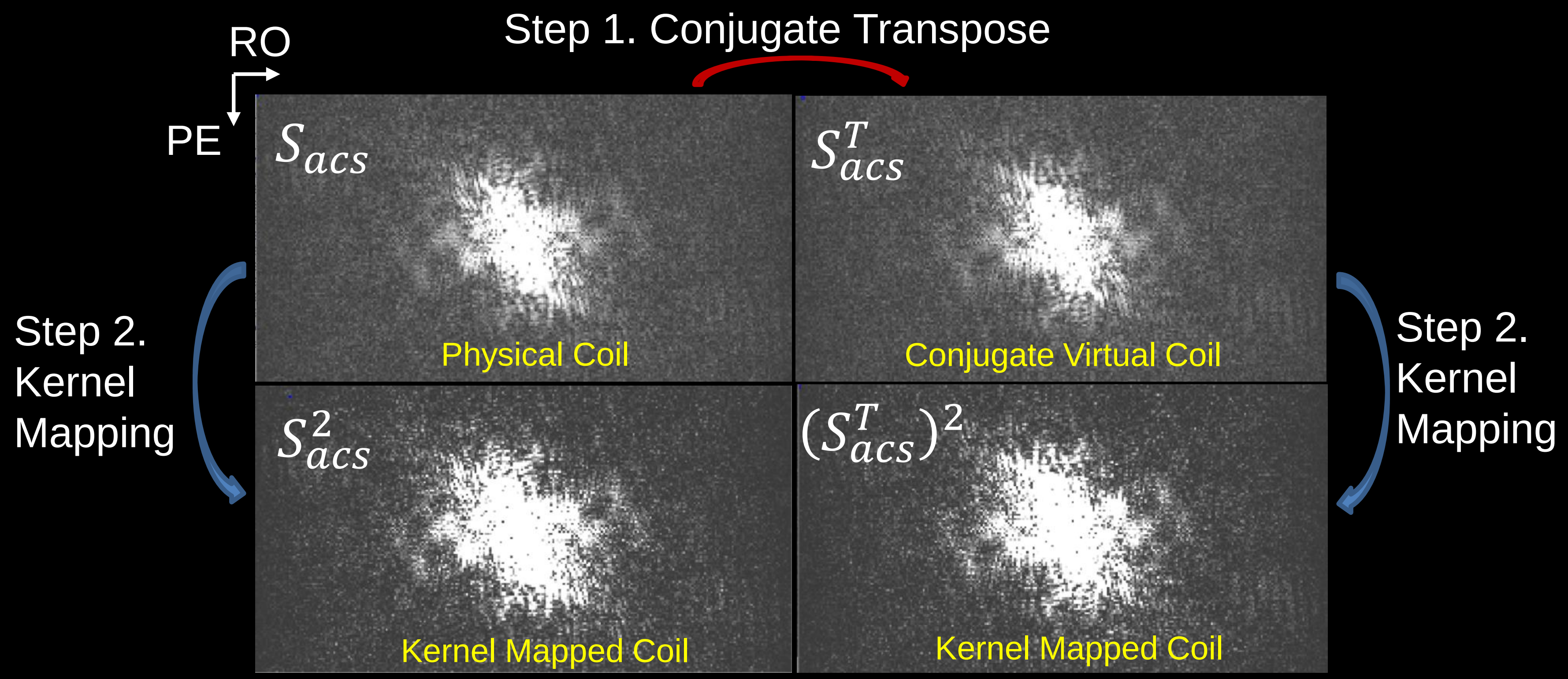

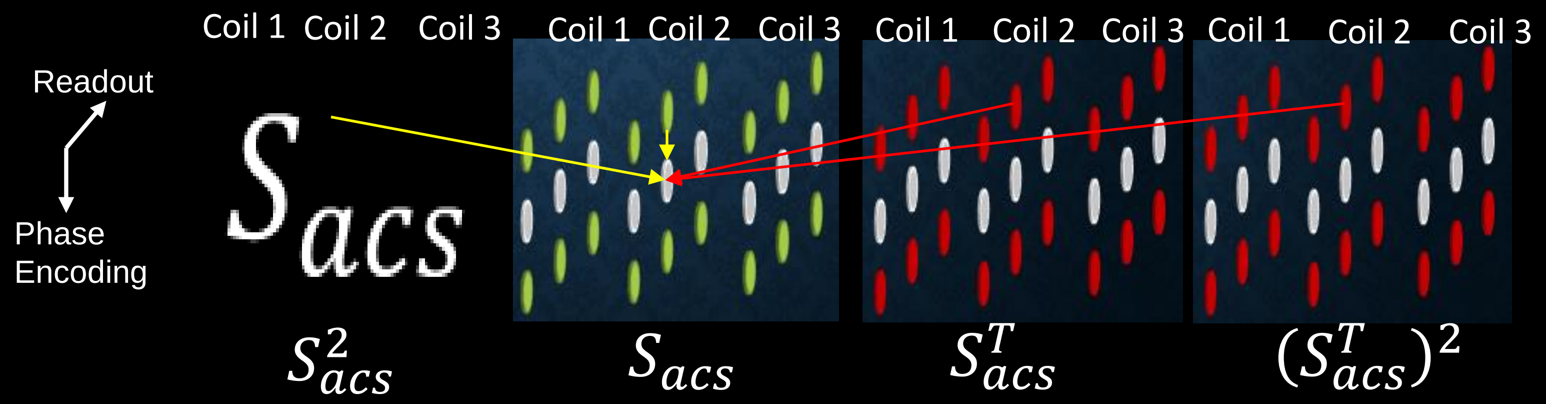

H Wang, S Jia & D Liang et al. PMB

CarRace accelerated Real-Time Cine

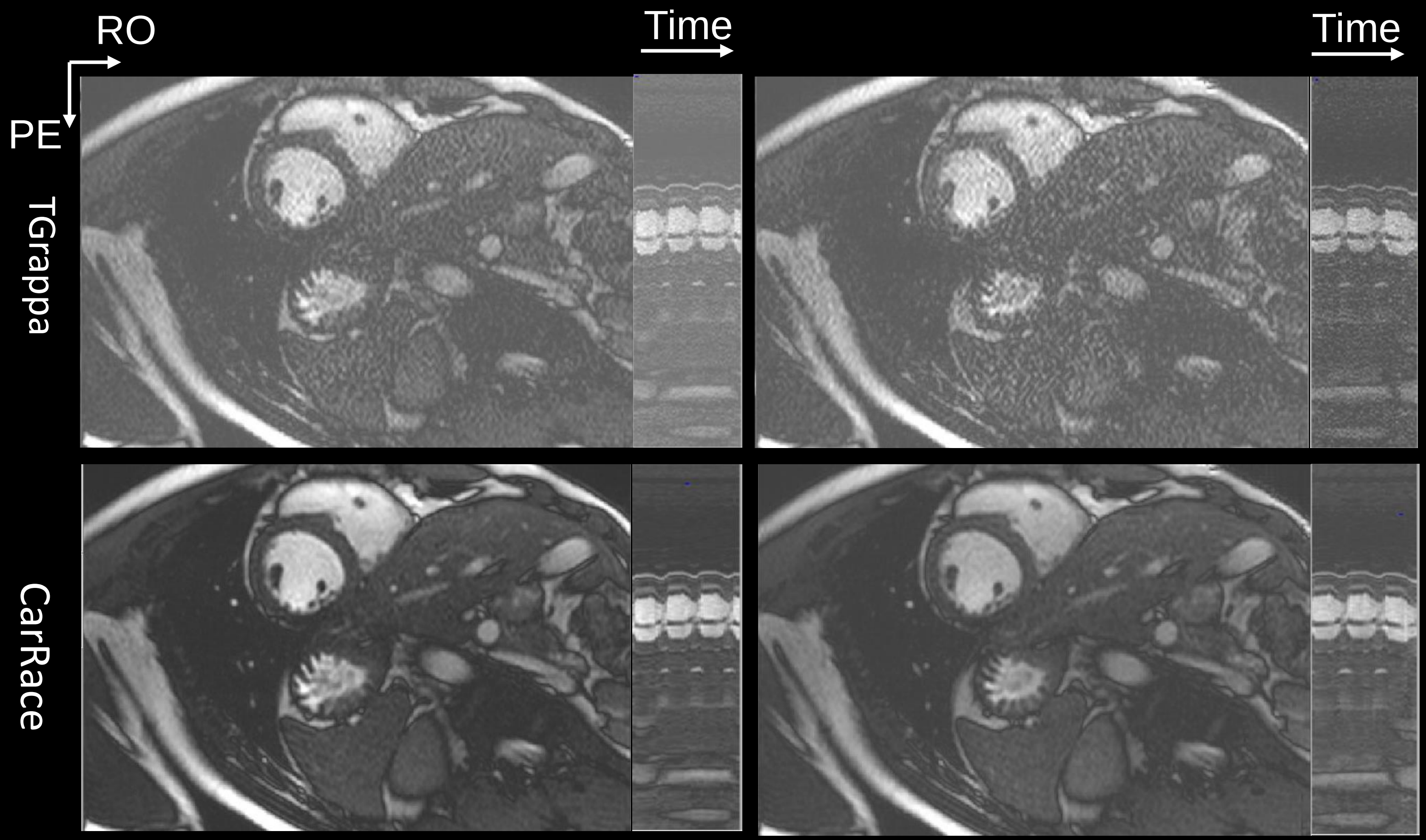

6X acceleration
192x192, 1.8 x 1.8 mm

8X acceleration
192x192, 1.8 x 1.8 mm

Submitted to MRM

CarRace: accelerated Real-Time Cine

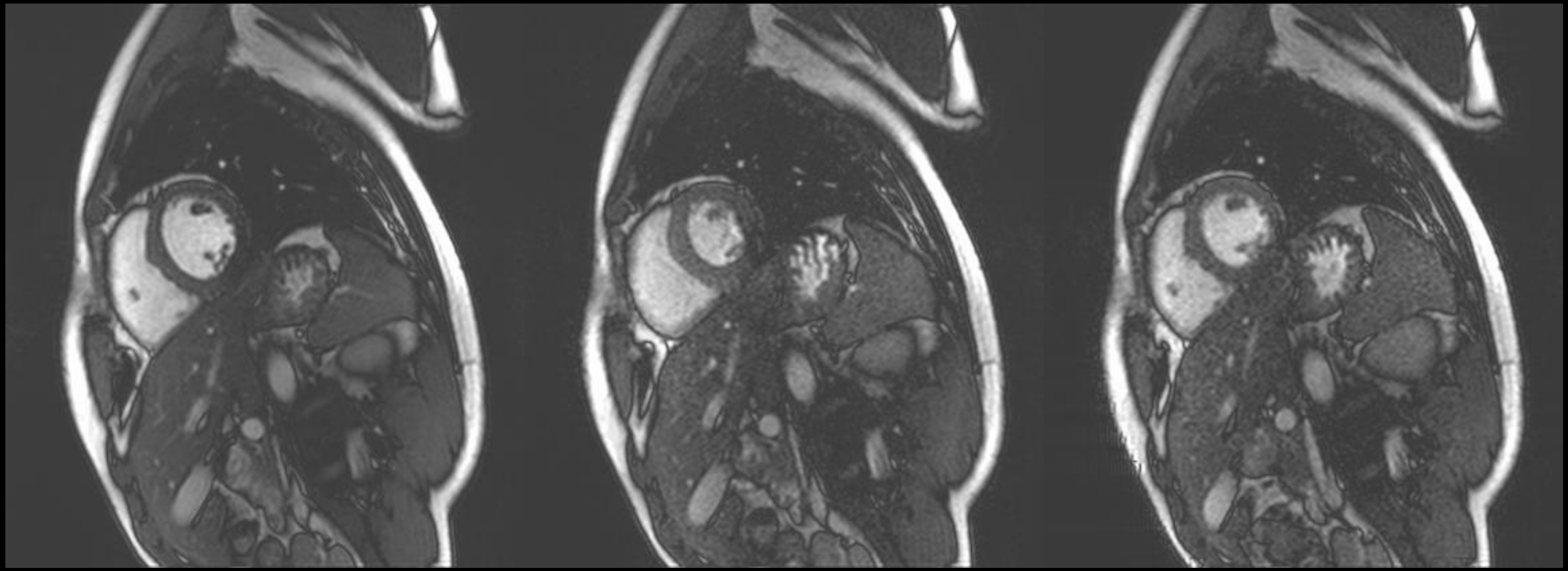

4X， ~85 ms/frame

6X, ~56 ms/frame

8X, ~40 ms/frame

Sparse Sampling based on compressed sensing

Compressed Sensing (CS):The sparse signals can be reconstructed accurately from very few incoherent measurements by a non-linear

ISMRM 20TH ANNUAL MEETING & EXHIBITION "Adapting MR in a Changing World" 5–11 MAY 2012 Melbourne AUSTRALIA

PLENARY SESSION

Imaging innovation: how compressed sensing would change the world of magnetic resonance

How Compressed Sensing will Change the World of MR
Organizers: Craig H. Meyer, Ph.D. & Daniel K. Sodickson, M.D., Ph.D.

07:30 Welcome & Awards - Debiao Li, Ph.D., 2011-12 ISMRM President

08:20 Lauterbur Lecture: MRI: From Science to Society, Vivian S. Lee, M.D., Ph.D., M.B.A.

09:05 *Compressed Sensing Overview*, David Donoho, Ph.D.

09:30 *Compressed Sensing in MRI*, Michael Lustig, Ph.D.

09:55 *Clinical Applications of Compressed Sensing: Introduction: Clinical Opportunities & Barriers to Mainstream Use*, Shreyas S. Vasanawala, M.D., Ph.D.

10:05 Case 1: *Sparse Neuroangiogram*, Manal Nicolas-Jilwan, M.D.

10:10 Case 2: *High Spatiotemporal Correlation Cardiac Imaging*, Jeanette Schulz-Menger, M.D.

10:15 Adjourn

CS-MRI

$$\min_{I} \| \Psi I \|_1 \quad \text{s.t.} \quad \| F_p I - f \|_2 < \varepsilon$$

F_p **:** CS encoding matrix

I **:** image to be reconstructed

Ψ **:** sparse transform

f **:** undersampled k-space data

$$\min_{I,D,\Gamma^{(i)}} \left\{ \sum_{l} \left\| D\alpha_l^{(i)} - R_l I \right\|_2^2 + \frac{\nu_1}{2} \left\| F_p I - f \right\|^2 \right\}$$

$$s.t. \quad \left\| \alpha_l^{(i)} \right\|_0 \leq T_0, \forall l$$

D **:** Adaptive dictionary

R_l **:** Extracted *l*th image patch

α_l **:** Sparse representation corresponding to *l*th patch

Sparsity in MR Images

Most MRI images are sparse or can be sparsely represented in some bases

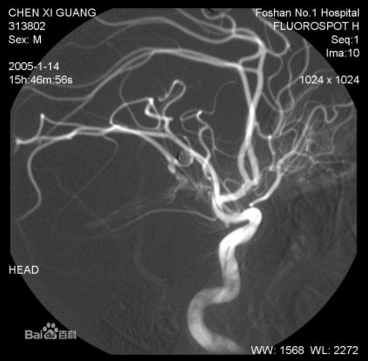

MR Angiography

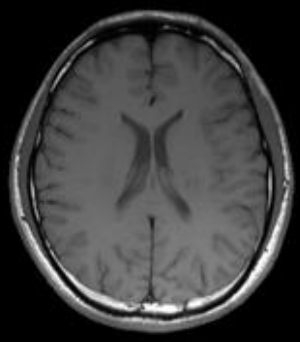

Brain

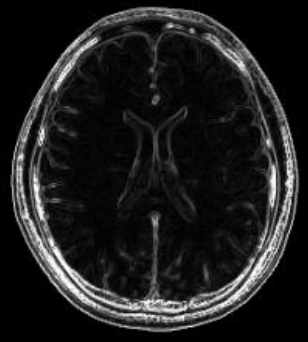

Finite Difference/TV

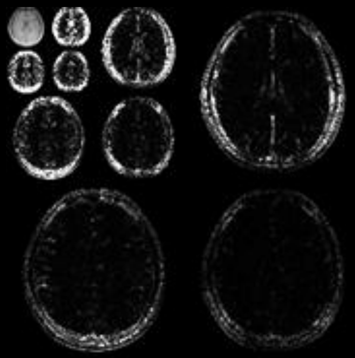

Wavelet

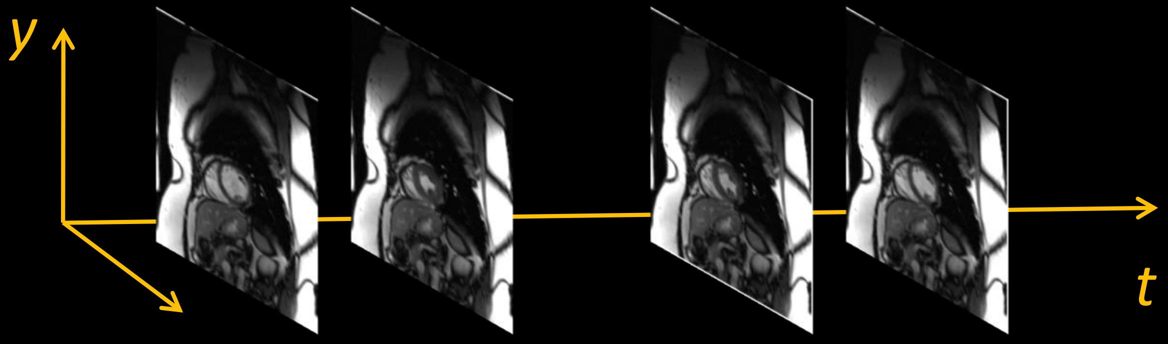

Cardiac cine

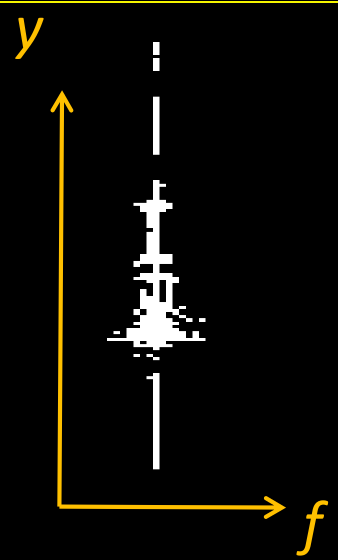

Temporal-frequency

Incoherence

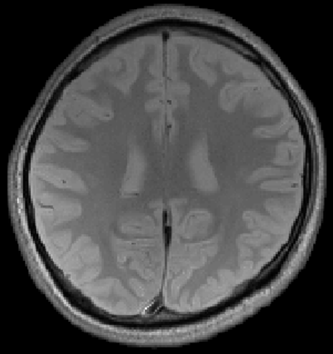

Image

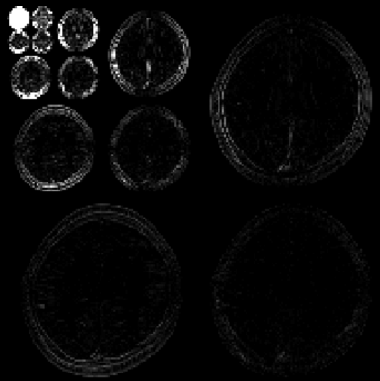

Sparse transform

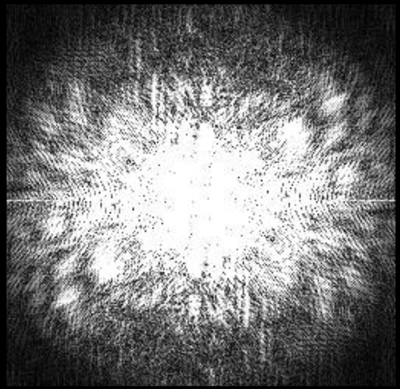

K-space

- **artifacts caused by incoherent undersampling are similar to noise**

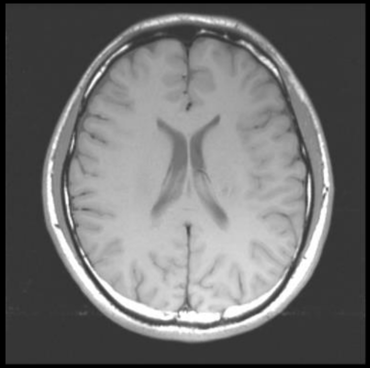

Image by
full sampling

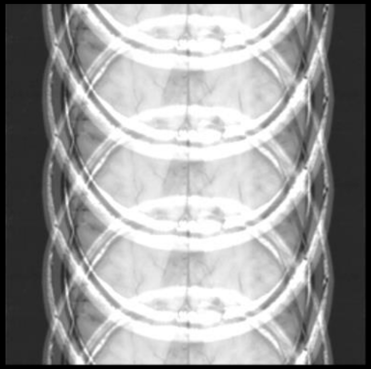

artifacts by
coherent sampling

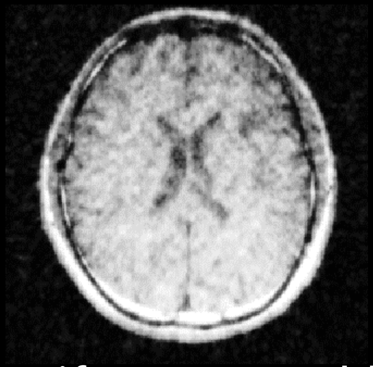

artifacts caused by
Incoherent sampling

Some Issues in CS-based MR Imaging

- **Long reconstruction time**
- **Complicated parameter-selection**
- **Losing fine details (“feature”)**

Gold standard (full sampled data)

CS(R=2.5, 1D variable density)

[1] S.Ravishankar et.al., IEEE TMI,2011 [2] Q. Liu, et.al., IEEE TIP,2013. [3] D. Liang et.al., MRM 2011. [4] V.Patel et.al., IEEE TIP 2012. [5] B. Ning et.al., MRI 2013

Long Reconstruction Time

Reason: nonlinear model, iterative reconstruction

Solution: 1) improve computing power

2) use pre-conditioner

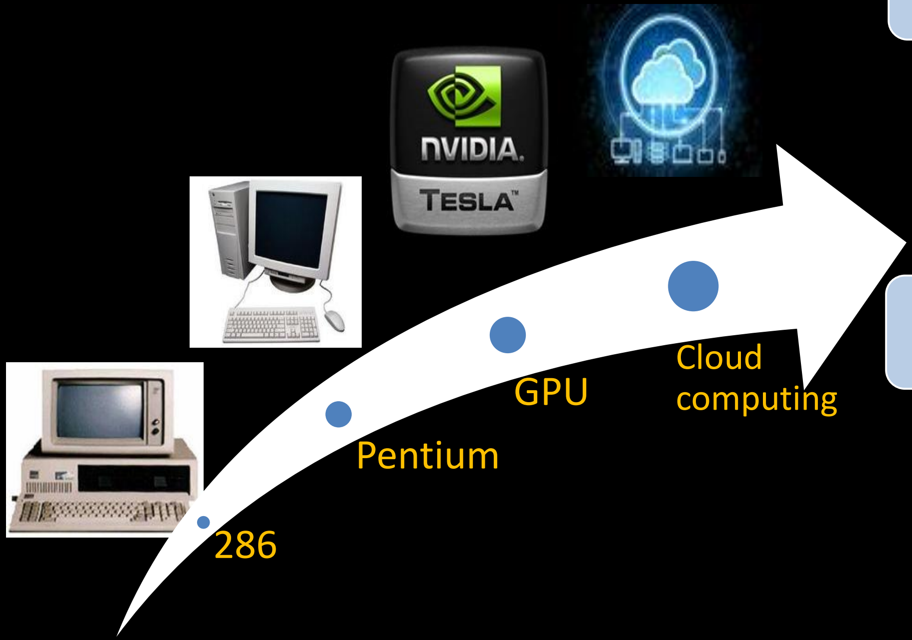

Diagonal pre-conditioner

$$P = \operatorname{argmin}_{P\text{diagonal}} \|PAA^* - I\|_F^2$$

$$u^{n+1} = (I + \sigma P)^{-1}(u^n + \sigma P(A(2x^n - x^{n-1}) + y))$$

$$x^{n+1} = \operatorname{prox}_{\tau g}(x^n - \tau A^* u^{n+1})$$

Circulant pre-conditioner

$$\mathbf{Ax} = \mathbf{b}$$

$$\mathrm{A} = \mu \sum_{i=1}^{N_c} (\mathrm{RFS}_i)^H \mathrm{RFS}_i + \lambda \left(\mathrm{D}_x^H \mathrm{D}_x + \mathrm{D}_y^H \mathrm{D}_y\right) + \gamma \mathrm{W}^H \mathrm{W}$$

$$\mathrm{A} = \mathrm{F}^H \mathrm{F} \mathrm{A} \mathrm{F}^H \mathrm{F} = \mathrm{F}^H \mathrm{K} \mathrm{F}$$

$$\mathrm{K} = \underbrace{\mu \sum_{i=1}^{N_c} \mathrm{FS}_i^H \mathrm{F}^H \mathrm{R}^H \mathrm{RFS}_i \mathrm{F}^H}_{\mathrm{K}_c} + \underbrace{\lambda \mathrm{F} \left(\mathrm{D}_x^H \mathrm{D}_x + \mathrm{D}_y^H \mathrm{D}_y\right) \mathrm{F}^H}_{\mathrm{K}_d} + \underbrace{\gamma \ \mathrm{I}}_{\mathrm{K}_w}$$

[1] F. Ong, et.al., ISMRM2018. [2] J. Gemert, et.al., ISMRM2018

Complicated Parameter-selection

Reason: **multi constraints， non-convex function**

Solution:

1) Test on a big data set and choose the sub-optimal but robust parameters

$$\min_{I} J(I) \quad \text{s.t.} \quad \left\| F_p I - f \right\|_2 \le \varepsilon$$

$$J(I) = \min_{D,\Gamma} \sum_{l} \left(\left\| \alpha_l \right\|_1 + \frac{\lambda}{2} \left\| D\alpha_l - R_l I \right\|_2^2 \right)$$

2) Parameter-free methods or automatic parameter selection

$$\begin{aligned} &\underset{\mathbf{x}}{\text{minimize}} && \|\mathbf{W}\mathbf{x}\|_1 \\ &\text{subject to} && \|\mathbf{y} - \mathbf{A}\mathbf{x}\|_2 \le \sigma\sqrt{n}, \end{aligned}$$

① Noise pre-scan
② First-order primal dual algorithm

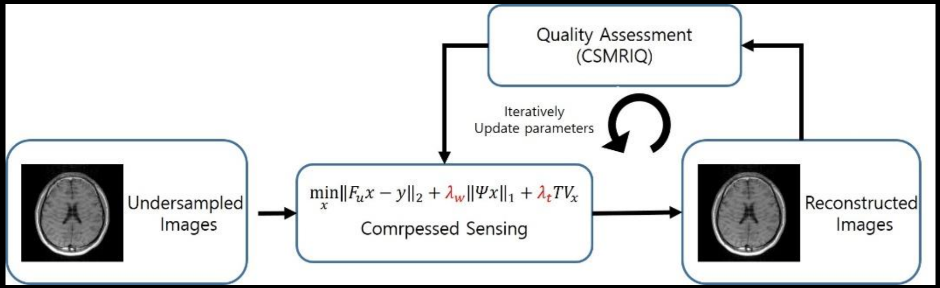

[1] K. Khare et al, MRM, 2013. [2] J. Tamir et al, ISMRM2018. [3] K. Bang et al, ISMRM2018. [4] J. Cheng et al, ISMRM2018

Loosing Details

Reason

$$\| I^{*} - I \|_2 \leq C_0 \| I - I_S \|_1 / \sqrt{S} + C_1 \varepsilon$$

I^{*} : Reconstruction solution I_S : Vector I with only S largest components

Details cannot be sparsely represented enough and are lost after nonlinear filtering

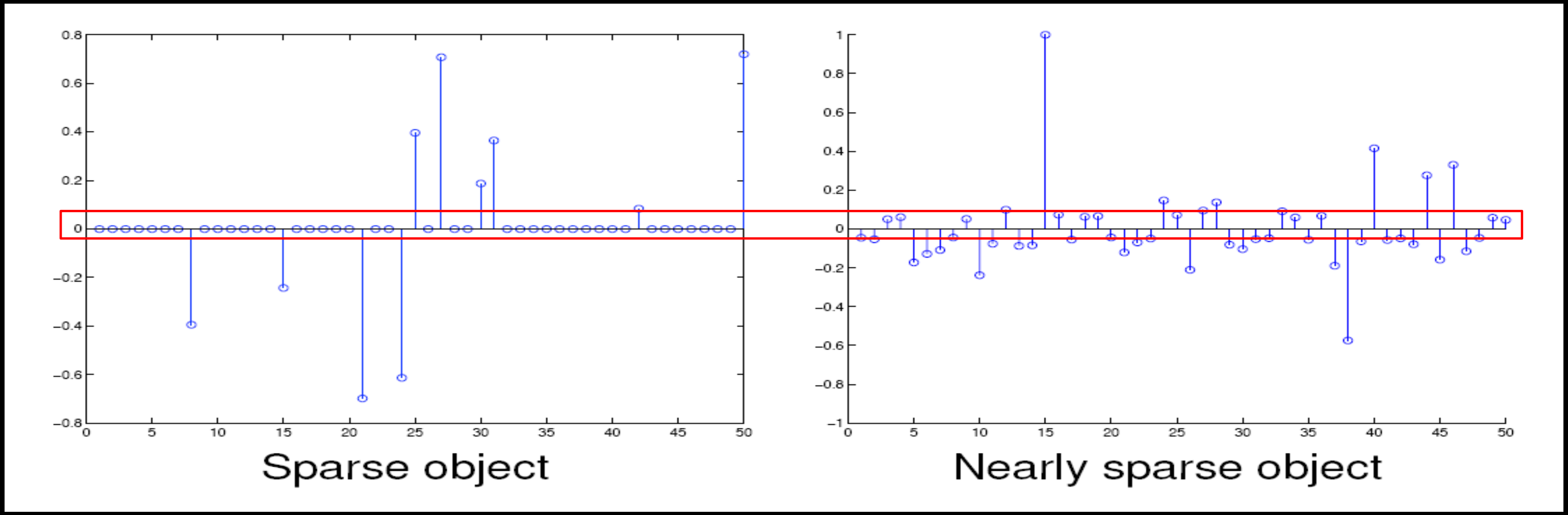

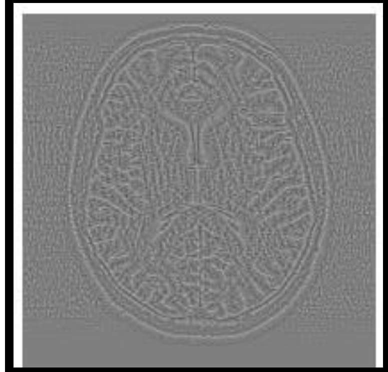

residual image

Candes, E. J et al, COMMUNICATIONS ON PURE AND APPLIED MATHEMATICS . 2006; 59 (8): 1207-1223

The methods of preserving details

Powerful sparse representation

- patch-based methods (dictionary learning, Nonlocal constraint)

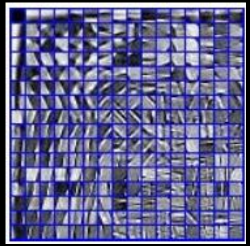

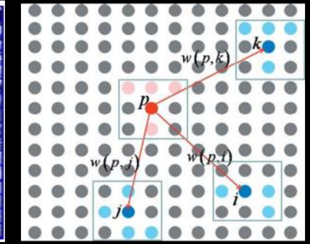

- Tensor-based Sparse transformation

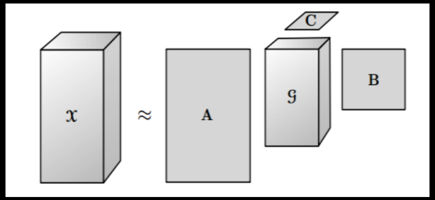

- Nonlinear compressed sensing method

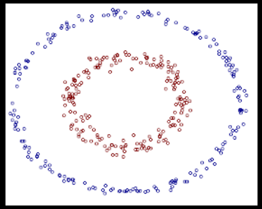

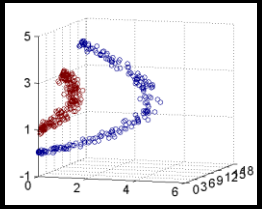

Detail restoration

- Iterative regularization method (IRM)

$$u_{k+1} = \arg\min_{u} \left(\| u \|_{L1} + \lambda \left\| I + v_k - u \right\|_2^2 \right)$$
$$v_{k+1} = v_k + I - u_{k+1}$$

- Bregman iterative method

$$I^{k+1} = \underset{I}{\operatorname{argmin}} \frac{1}{2} \| F_p I - f^k \|_2^2 + \lambda \| I \|_{L1}$$
$$f^{k+1} = f^k + f - F_p I^{k+1}$$

[1] S.Ravishankar et.al., IEEE TMI,2011 [2] Q. Liu, et.al., IEEE TIP,2013. [3] D. Liang et.al., MRM 2011. [4] S.Fang et.al., MRM 2010. [5] Y. Yu et.al., PLoS ONE,2014. [6] J He et.al., IEEE TMI,2016. [7] Y. Zhou , et.al., ISBI 2007.[8]http://blog.sina.com.cn/s/blog_89ba75c80101gxgm.html [9]S. Osher et.al, Multiscale Model. Simul., 2005. [10] B. Liu et.al., MRM, 2009. [11] W. Yin et.al., SIAM J. Imaging Sci., 2008. [12] X Ye et.al., IEEE TMI, 2011. [13] S. Wang et. al., PMB 2016. [14] J. Cheng et. al., MRM 2018

CS-MRI with Iterative Feature Refinement

Question: how to only get back the features , but throw away the noise and noise-like artifacts?

Solution: try to extract only features from the residual image and add back to the iteration

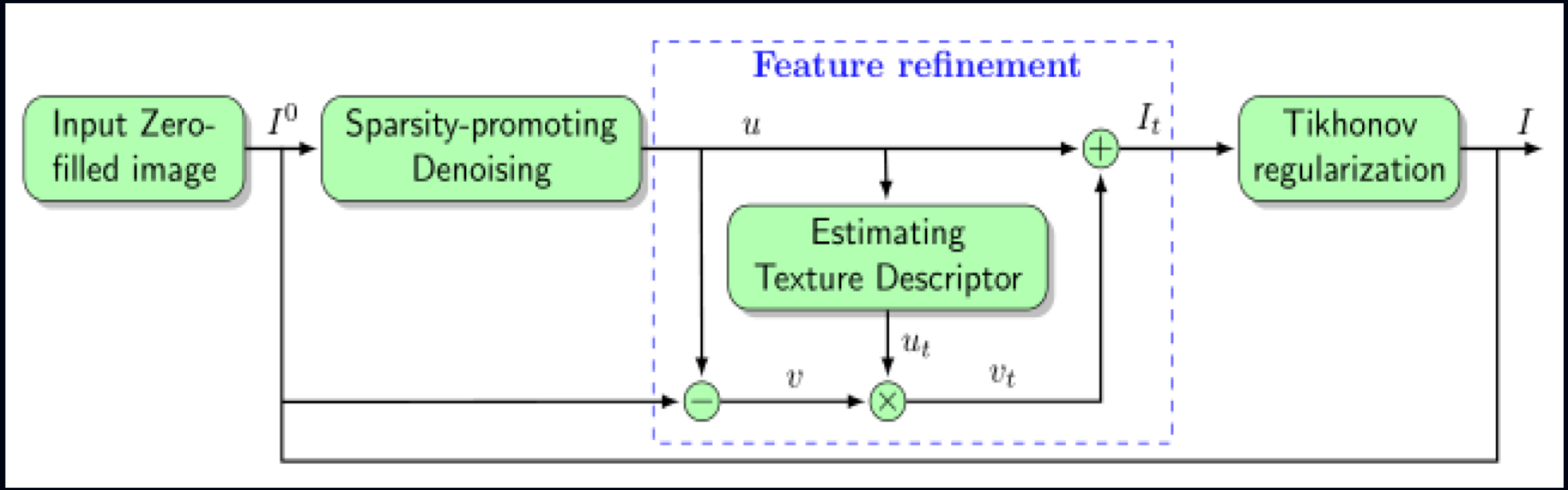

IFR-CS

A Close Look at the Iteration

Single iteration

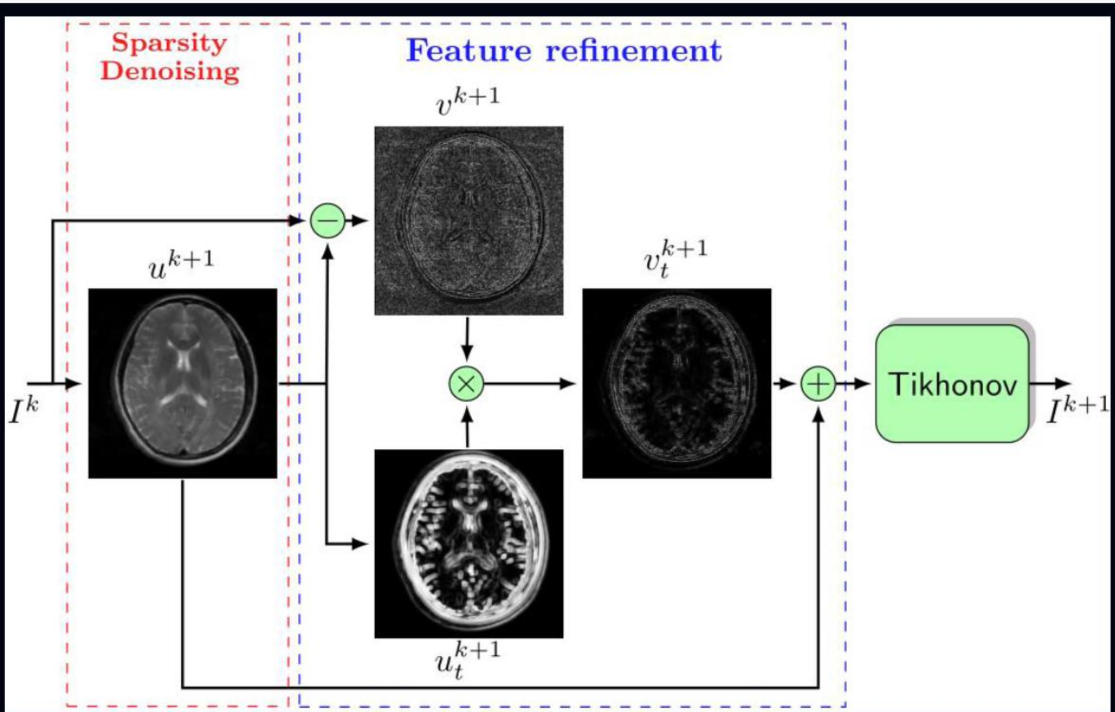

(a) I (b) u (c) v (d) I_t (e) $I - I_t$

input image | denoised image | residual image | denoised image w/ FR | residual image w/ FR

Physics in Medicine and Biology Highlights of 2016

Highlights of 2016

Welcome to the *Physics in Medicine and Biology* (PMB) Highlights of 2016 collection. This page brings together some of the very best research published in PMB in 2016, celebrating the quality and diversity of papers we published last year. Selected by the Editors, the articles featured span some of the most cutting-edge areas of biomedical physics, and collectively are a reflection of the most influential research published in PMB in 2016.

If you want to feature in the 2017 Highlights then submit your paper to PMB and you might see your work highlighted here next year. We hope that you find these highlights of interest. For more information about submitting your own research to PMB please e-mail the team at pmb@iop.org.

All articles listed below are **free-to-read** until 31 December 2017. You can also view the Highlights of 2015

Maggie Simmons
Publisher
Physics in Medicine and Biology

Iterative feature refinement for accurate undersampled MR image reconstruction

Shanshan Wang *et al* 2016 *Phys. Med. Biol.* **61** 3291

+ View abstract   View article   PDF

Editorial: the articles featured span some of the most cutting-edge areas and a reflection of the most influential research published in PMB 2016

Application: Whole Brain Vessel Wall Imaging

Stroke

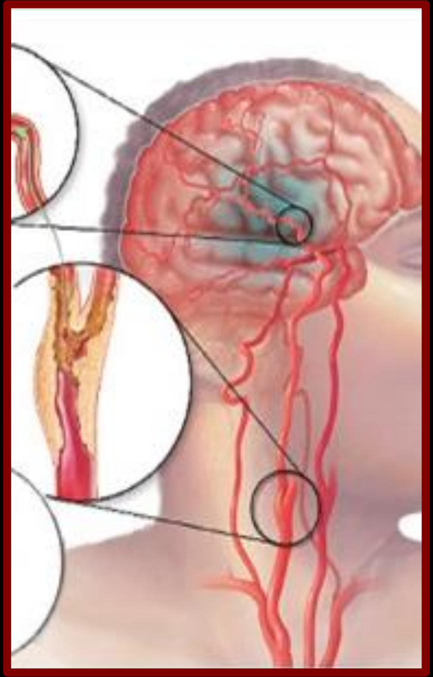

MR Angiography

MR VW imaging

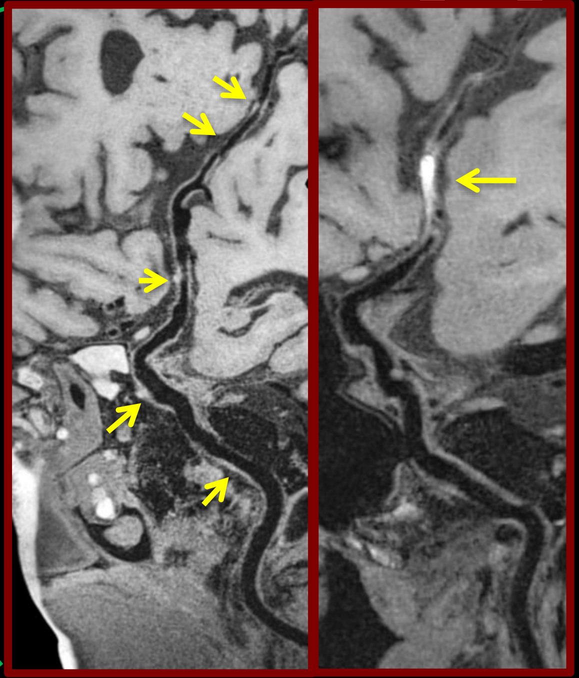

Challenges : high resolution, large FOV and fast scan

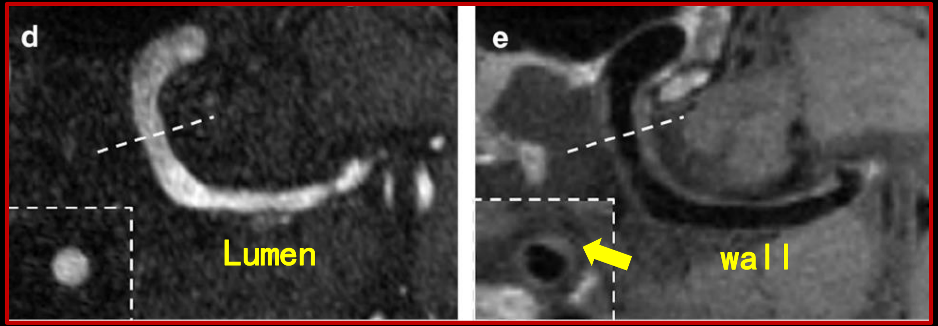

Current: 24min without acceleration , 9min with parallel imaging

5 mins： 3D Whole Brain Vessel Wall Imaging

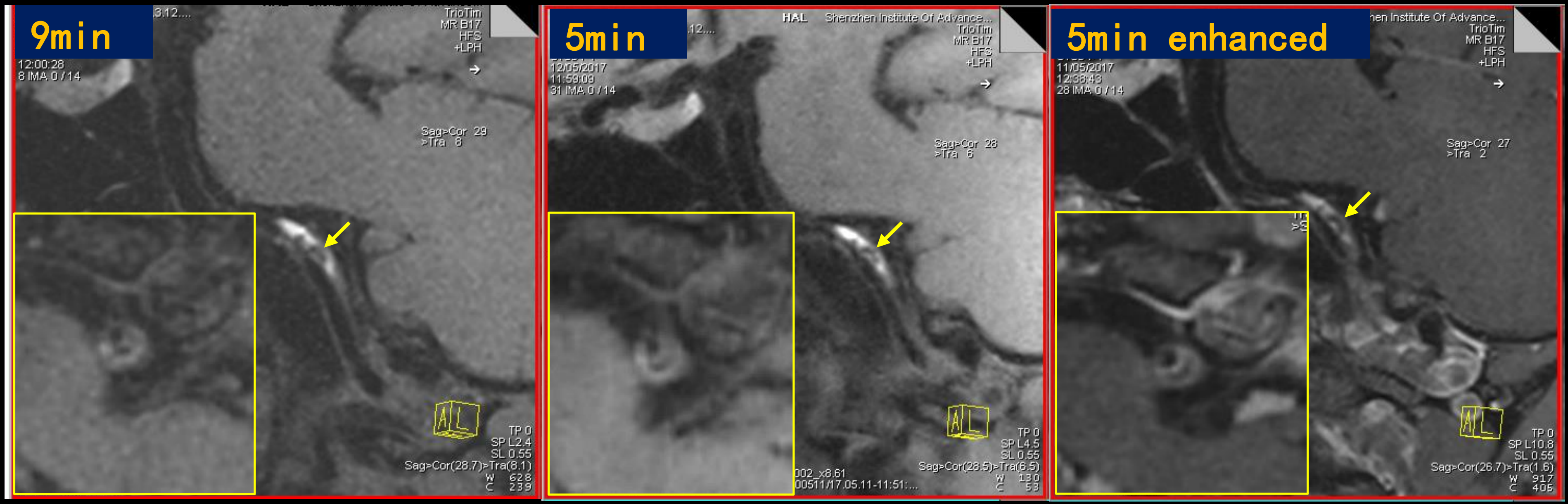

47y female patient， Arterial dissection is visible

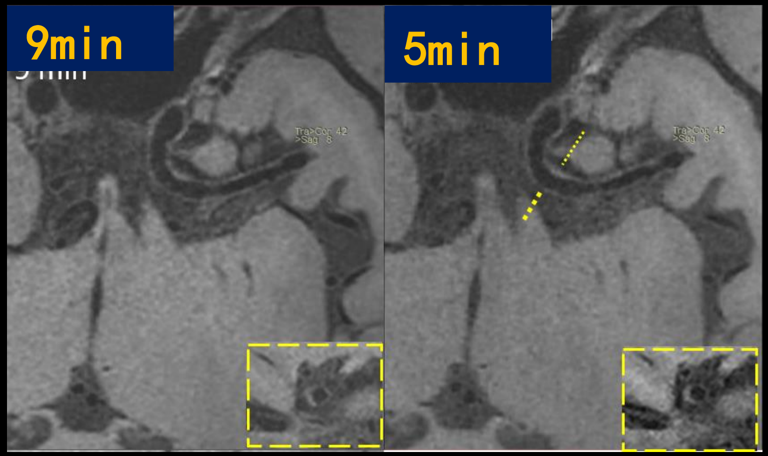

45y male stroke patient， eccentric thickening

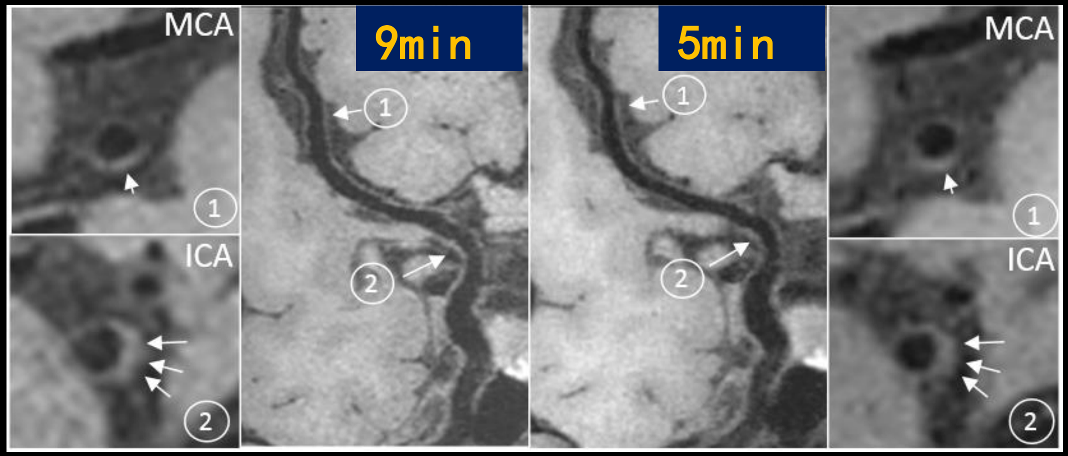

52y male stroke patient ， eccentric thickening

Joint Intracranial and Carotid Arterial Wall Imaging

Parallel Imaging 2.7x in 9:18 min

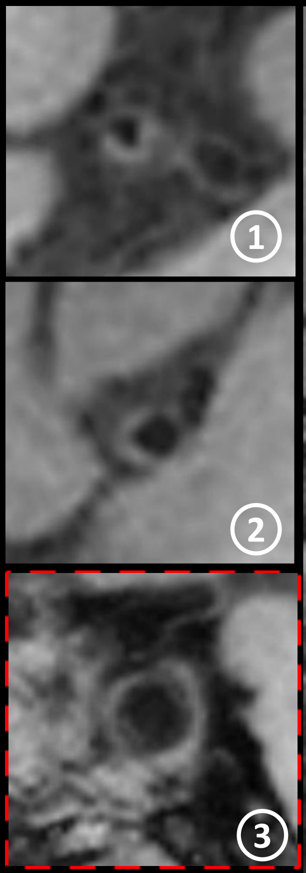

A female stroke patient of 47 years old.

Compressed Sensing 5x in 5 min 0.55mm

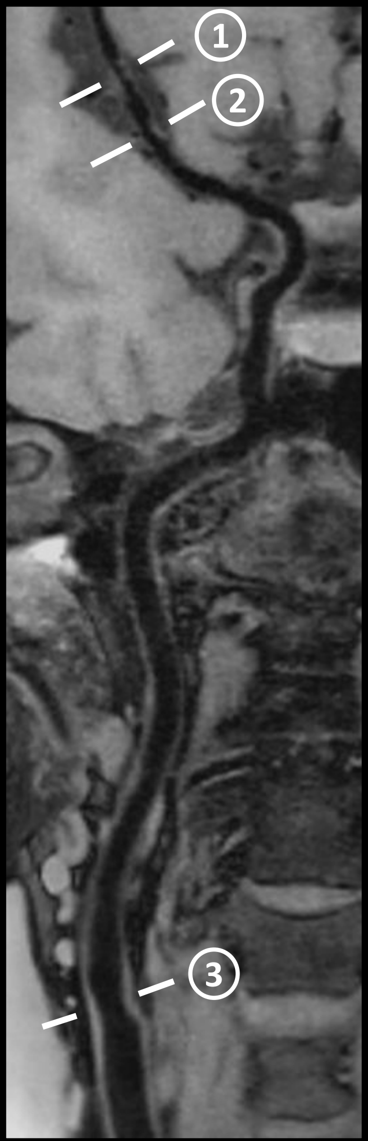

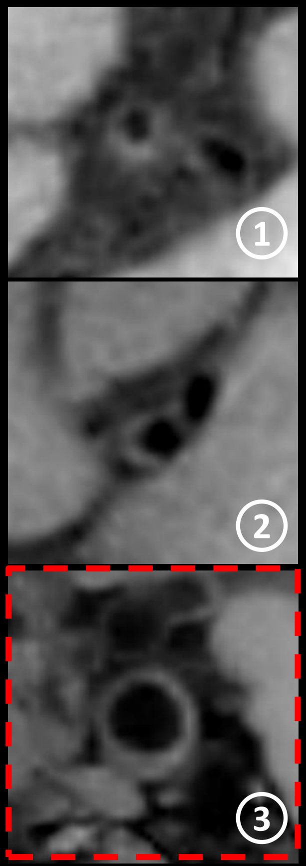

Wall thickening was detected in MCA and ECA.

Joint Intracranial and Carotid Arterial Wall Imaging

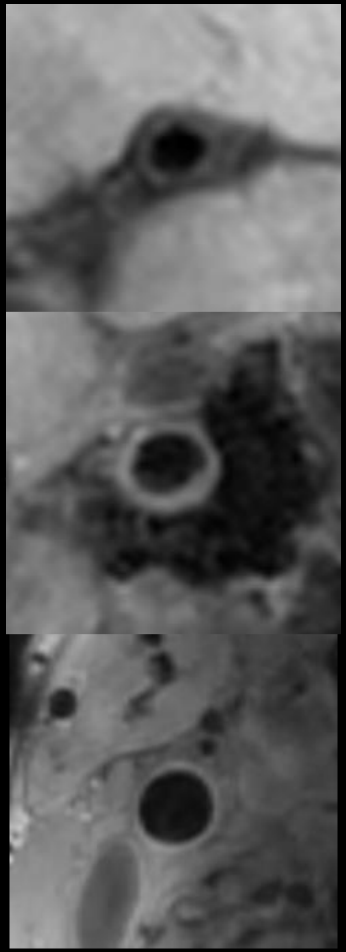

FOV：230 x 210 x 192 mm
Scan resolution：0.6 x 0.6 x 0.6 毫米
Coil：32-channel Head&Neck
TA：3.5mins
A 62-year old male

S. Jia et al. ISMRM2020

Collaboration with industry

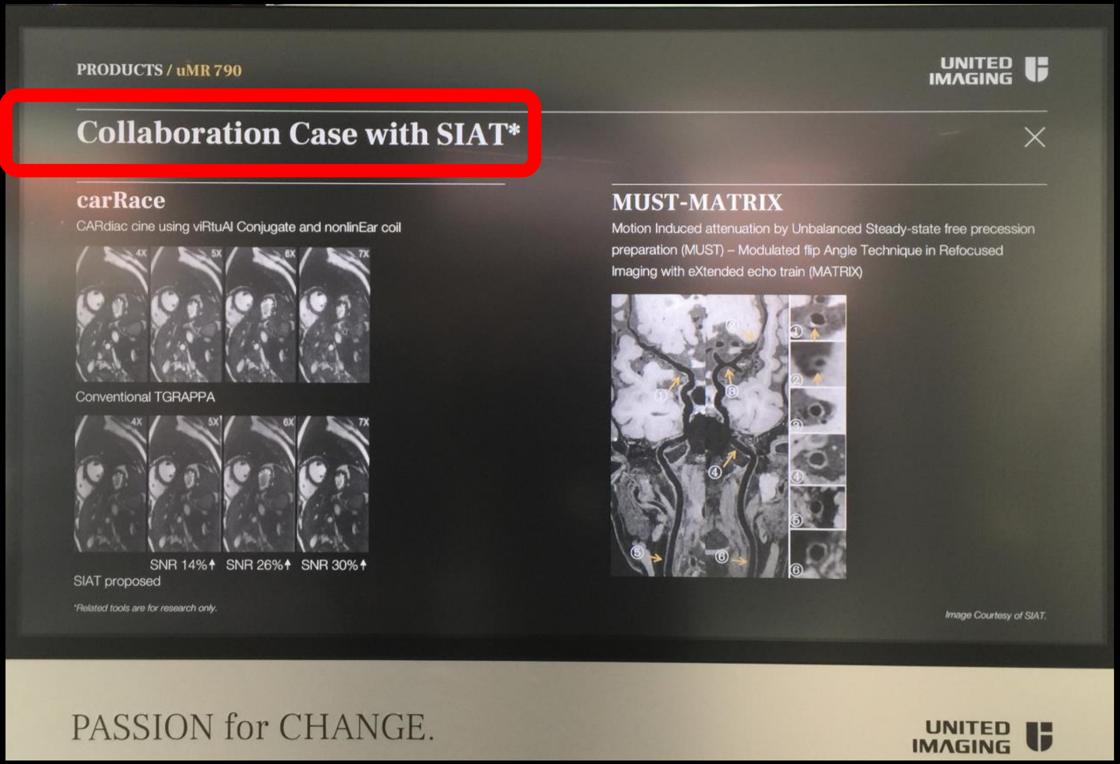

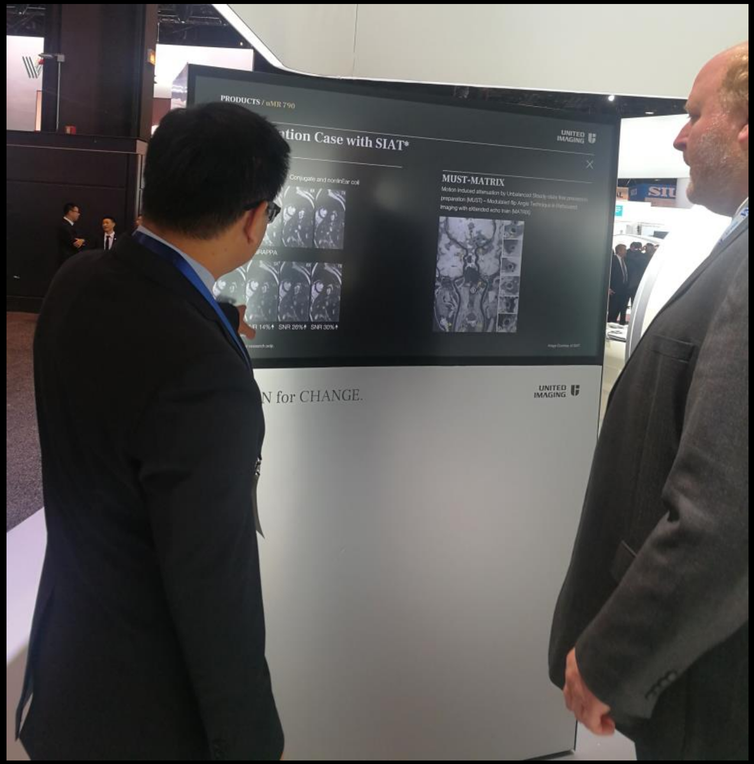

Ultrafast cardiac MR imaging and Vessel Wall Imaging were featured in the 2018 Radiological Society of North America (RSNA) as the highlight of the cooperation between SIAT and United Imaging (UI).

Deep Learning MRI: motivation

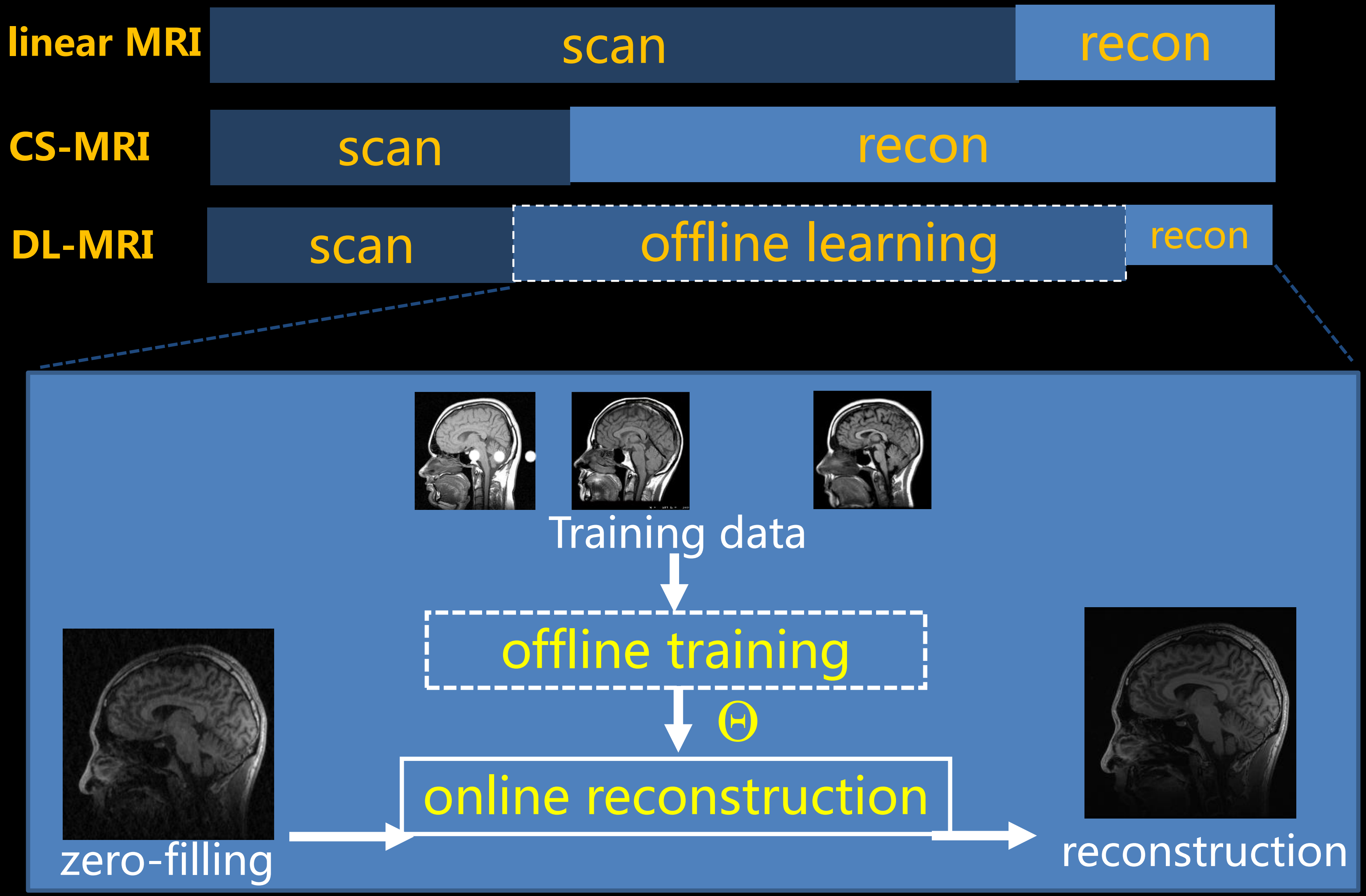

Fast recon
Learn parameters

Deep Learning MRI : Preliminary work

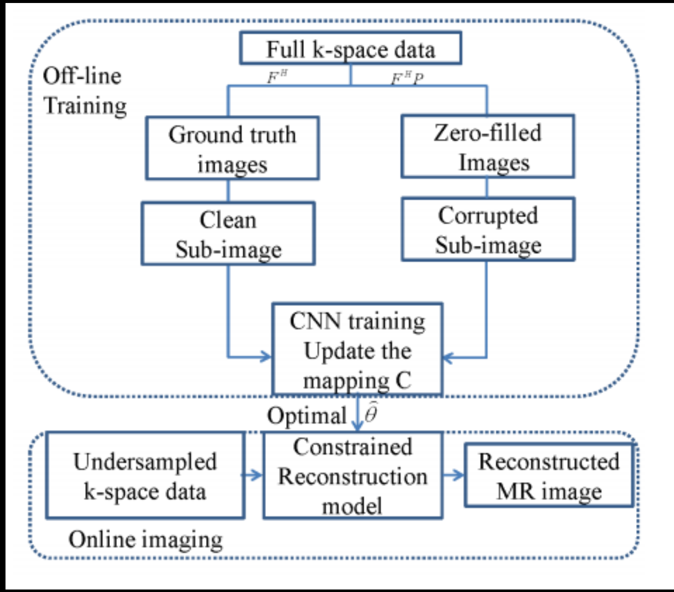

1. S Wang, L. Ying, D Liang, "Accelerating Magnetic ResonanceImaging via Deep Learning," IEEE-ISBI 2016: 514-517.

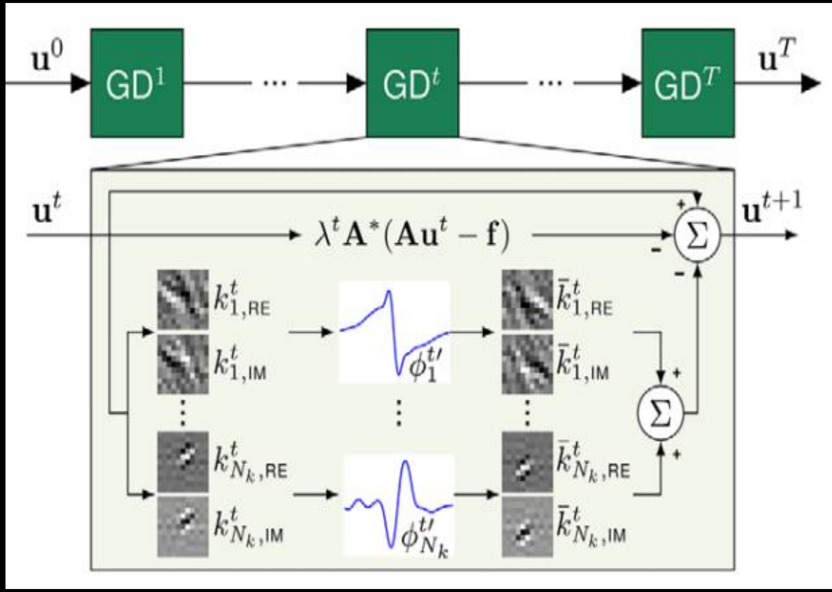

2. Hammernik K, et al. Learning a Variational Network for Reconstruction of Accelerated MRI Data. ISMRM 2016.

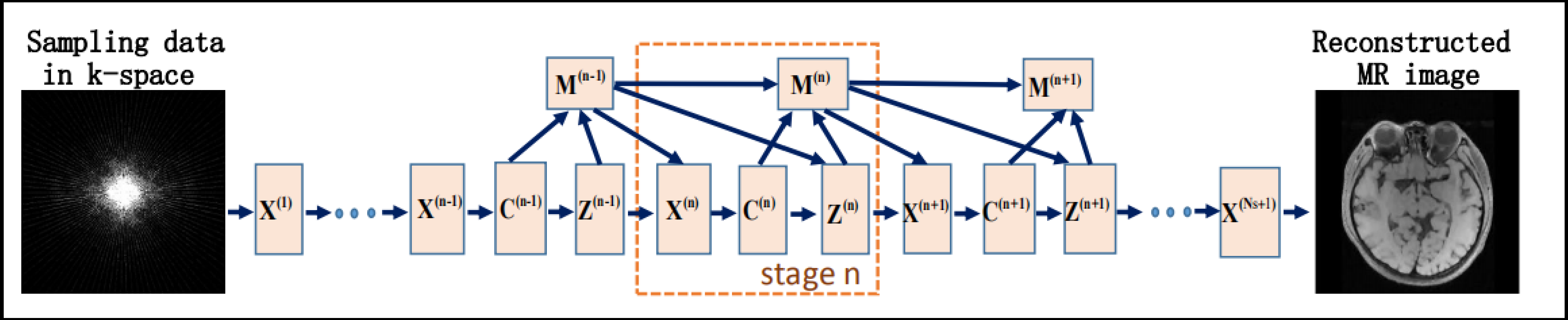

3. Yang Y , Sun J, Li H, Xu Z. Deep ADMM-net for compressive sensing MRI. Advances in Neural Information Processing Systems 2016: 10-18.

Deep Learning MRI: Our Roadmap

梁栋（Dong Liang），朱燕杰，吴垠，刘新，郑海荣，基于机器学习的并行磁共振成像GRAPPA方法，ZL201210288373.4

已转让上海联影

Dong Liang et al, Machine learning for GRAPPA, ZL201210288373.4

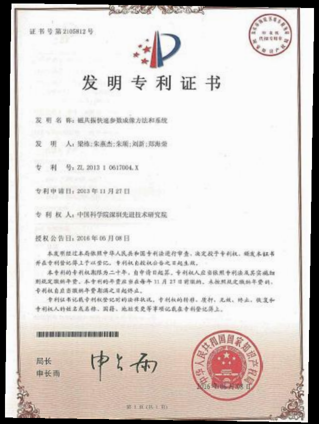

梁栋（Dong Liang），朱燕杰，朱顺，刘新，郑海荣，基于深度学习的磁共振快速参数成像方法和系统，ZL201310617004.X

Dong Liang et al, Deep learning for fast parameter mapping, ZL201310617004.X

梁栋（Dong Liang），朱燕杰，朱顺，刘新，郑海荣，基于深度学习的磁共振成像方法和系统，ZL201310633874.6

Dong Liang et al, Deep learning for fast MR imaging ZL201310617004.X

Deep Learning for Fast MR Imaging

D Liang et al., IEEE Sig Proc Mag, 37(1):141-151, 2020

Linear MRI	Scan		**Recon**
CS-MRI	Scan	**Recon**	
DL-MRI	Scan	Learning	Recon

Data-driven

input →  → **output**

Offline Training

Training data

Model-driven

Iterative procedure of an algorithm

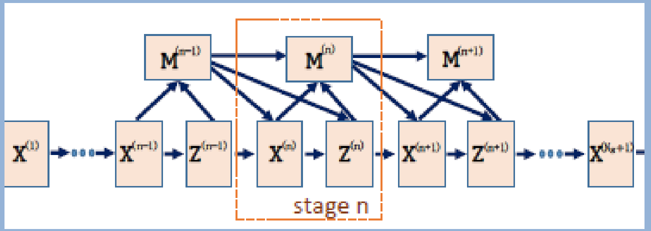

Offline Training

Training data

Model-driven Deep Learning

$$\|Ax - f\|_2^2 + \lambda \|F(x)\|_1$$

$$\begin{cases} r^{(n+1)} = x^{(n)} - \rho A^T\left(Ax^{(n)} - f\right) \\ x^{(n+1)} = \tilde{F}\left(soft\left(F\left(r^{(n+1)}\right), \theta\right)\right) \end{cases}$$

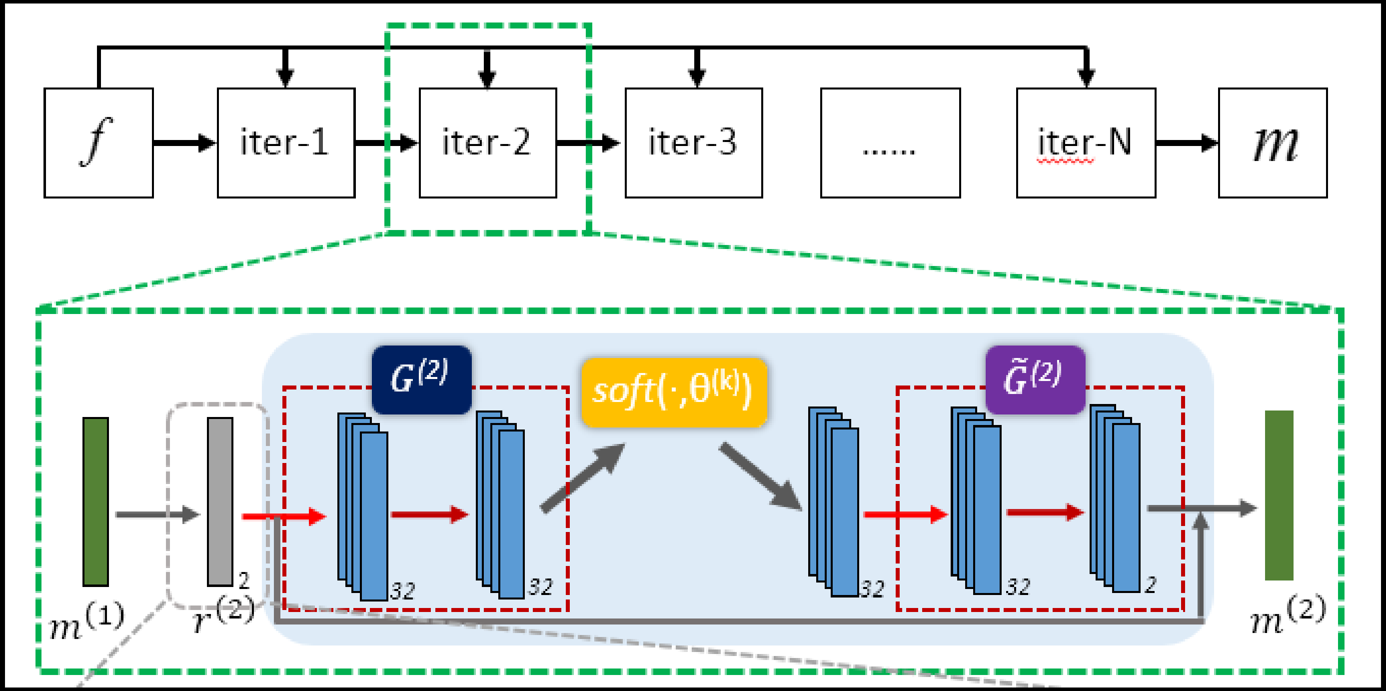

Model-driven Deep Learning

Unrolling the iterations of an optimization algorithm to deep network

Learning capability of deep networks

Convergence guarantee of optimization algorithms

$$\frac{1}{2}\|Ax-f\|_2^2+\lambda\|\Psi x\|_1$$

$$\frac{1}{2}\|Ax-f\|_2^2+\lambda R(x)$$

$$d(Ax, f)+\lambda R(x)$$

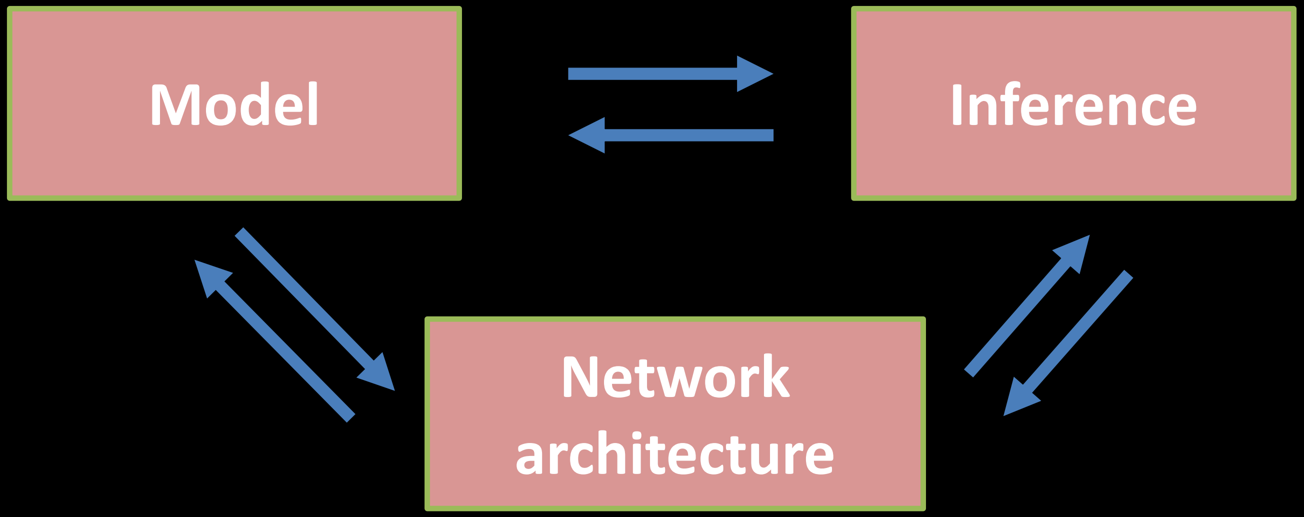

- Gradient decent
- ADMM
- FISTA
- PDHG
- …

- CNN
- RNN
- GAN
- …

A could be Fourier encoding or sensitivity encoding (learnable)

Relaxing Constraints in Model-driven Deep Learning

Data-driven

Learning the inverse mapping $\Gamma(f)$

Learning the variable structures in the algorithm

Learning data fidelity $\|\cdot\|_2^2$ → $d(Ax, f) + \lambda R(x)$

Learning regularizer $\|\cdot\|_1$ → $\frac{1}{2}\|Ax - f\|_2^2 + \lambda R(x)$

Learning transform Ψ → $\frac{1}{2}\|Ax - f\|_2^2 + \lambda\|D(x)\|_1$

Learning parameters λ → $\frac{1}{2}\|Ax - f\|_2^2 + \lambda\|\Psi x\|_1$

More training data

Model-driven

VN (Variational Network)

$$\min\|Ax-y\|_2^2+\sum_{i=1}^{N_k}\langle\Phi_i(\mathrm{K}_i x),1\rangle$$

Parameters
Transform
Regularizer

Gradient Decent

$$u^{n+1}=u^n-\sum_{i=1}^{N_k}(K_i^n)^T\Phi_i^{n\prime}(K_i^n u^n)-\lambda^n A^*(Au^n-y)$$

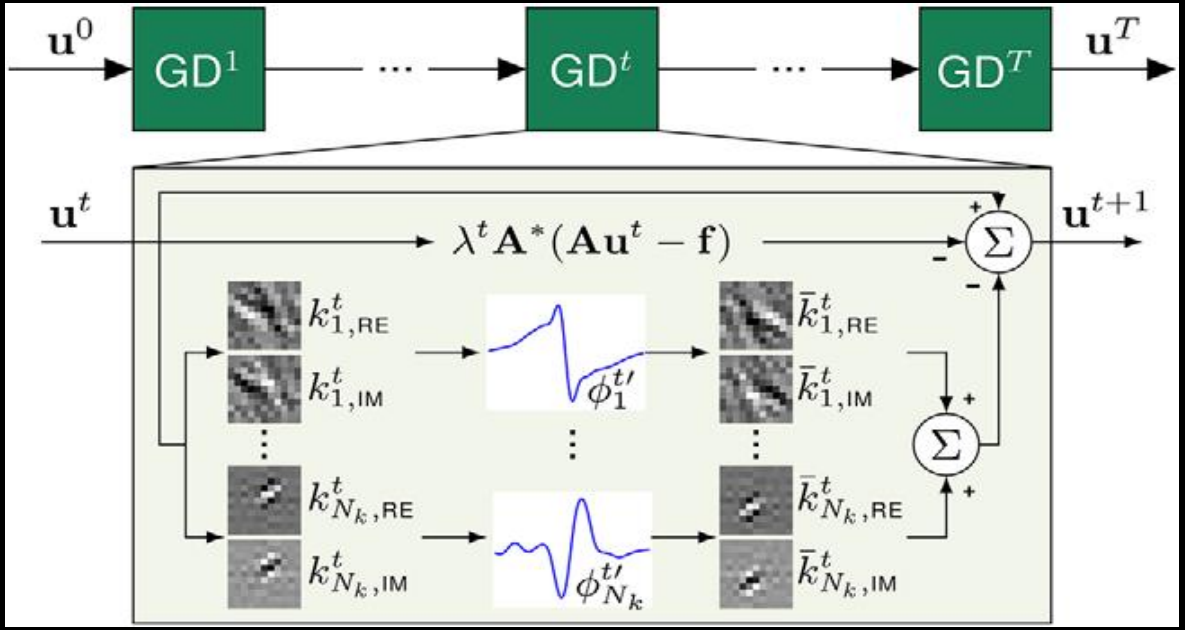

K. Hammernik et al. MRM2018

ADMM-CSnet

$$\min \|Ax - y\|_2^2 + \sum_{l=1}^{L} \lambda_l \, g(D_l x)$$

Parameters
Transform
Regularizer

ADMM Solver 1 $z_l = D_l x$ **Transform domain**

$$\begin{cases} X^{(n)}: x^{(n)} = \dfrac{\left[A^H y + \sum_{l=1}^{L} \rho_l D_l^T \left(z_l^{(n-1)} - \beta_l^{(n-1)}\right)\right]}{\left[A^H A + \sum_{l=1}^{L} \rho_l D_l^T D_l\right]} \\ Z^{(n)}: z_l^{(n)} = S\left(D_l x^{(n)} + \beta_l^{(n-1)}; \lambda_l / \rho_l\right) \\ M^{(n)}: \beta_l^{(n)} = \beta_l^{(n-1)} + \eta_l \left(D_l x^{(n)} - z_l^{(n)}\right) \end{cases}$$

Basic-ADMM-CSNet

Learnable

ADMM Solver 2 $Z = X$ **Image domain**

$$\begin{cases} X^{(n)}: x^{(n)} = \dfrac{\left[A^H y + \rho\left(z^{(n-1)} - \beta^{(n-1)}\right)\right]}{\left(A^H A + \rho I\right)} \\ Z^{(n)}: z^{(n)} = \mu_1 z^{(n,k-1)} + \mu_2 \left(x^{(n)} + \beta^{(n-1)}\right) \\ \quad - \sum_{l=1}^{L} \tilde{\lambda}_l D_l^T H\left(D_l z^{(n,k-1)}\right) \\ M^{(n)}: \beta^{(n)} = \beta^{(n-1)} + \tilde{\eta}\left(x^{(n)} - z^{(n)}\right) \end{cases}$$

Generic-ADMM-CSNet

Y Yang, J Sun, Z Xu et al. NIPS 2006,IEEE TPRMI 2018

ADMM-CSnet

ADMM-net- I

$$\|Ax - f\|_2^2 + \sum_{l=1}^{L} \lambda_l g(D_l x)$$

$$\begin{cases} X^{(n)}: x^{(n)} = \dfrac{\left[A^H f + \rho\left(z^{(n-1)} - \beta^{(n-1)}\right)\right]}{(A^H A + \rho I)} \\ Z^{(n)}: z^{(n)} = \mu_1 z^{(n,k-1)} + \mu_2\left(x^{(n)} + \beta^{(n-1)}\right) \\ \qquad - \sum_{l=1}^{L} \tilde{\lambda}_l D_l^T H\left(D_l z^{(n,k-1)}\right) \\ M^{(n)}: \beta^{(n)} = \beta^{(n-1)} + \tilde{\eta}\left(x^{(n)} - z^{(n)}\right) \end{cases}$$

Learning data consistency

ADMM-net- II

$$d(Ax, f) + \sum_{l=1}^{L} \lambda_l g(D_l x)$$

$$\begin{cases} X^{(n)}: x^{(n)} = m_1 x^{(n,k-1)} + m_2\left(z^{(n-1)} - \beta^{(n-1)}\right) \\ \qquad -\gamma A^H \Gamma(Ax^{(n,k-1)}, f) \\ Z^{(n)}: z^{(n)} = \mu_1 z^{(n,k-1)} + \mu_2\left(x^{(n)} + \beta^{(n-1)}\right) \\ \qquad - \sum_{l=1}^{L} \tilde{\lambda}_l D_l^T H\left(D_l z^{(n,k-1)}\right) \\ M^{(n)}: \beta^{(n)} = \beta^{(n-1)} + \tilde{\eta}\left(x^{(n)} - z^{(n)}\right) \end{cases}$$

Learning variable structures

ADMM-net-III

$$d(Ax, f) + \lambda R(x)$$

$$\begin{cases} D^{(n)}: d^{(n)} = \Gamma(Ax^{(n-1)}, f) \\ X^{(n)}: x^{(n)} = \Pi(x^{(n-1)}, z^{(n-1)} - \beta^{(n-1)}, A^H d^{(n)}) \\ Z^{(n)}: z^{(n)} = \Lambda\left(x^{(n)} + \beta^{(n-1)}\right) \\ M^{(n)}: \beta^{(n)} = \beta^{(n-1)} + \tilde{\eta}\left(x^{(n)} - z^{(n)}\right) \end{cases}$$

[1] Y Yang et al. IEEE TPRMI 2018

[2] J Cheng and D Liang. unpublished data

ADMM-CSnet

R=6

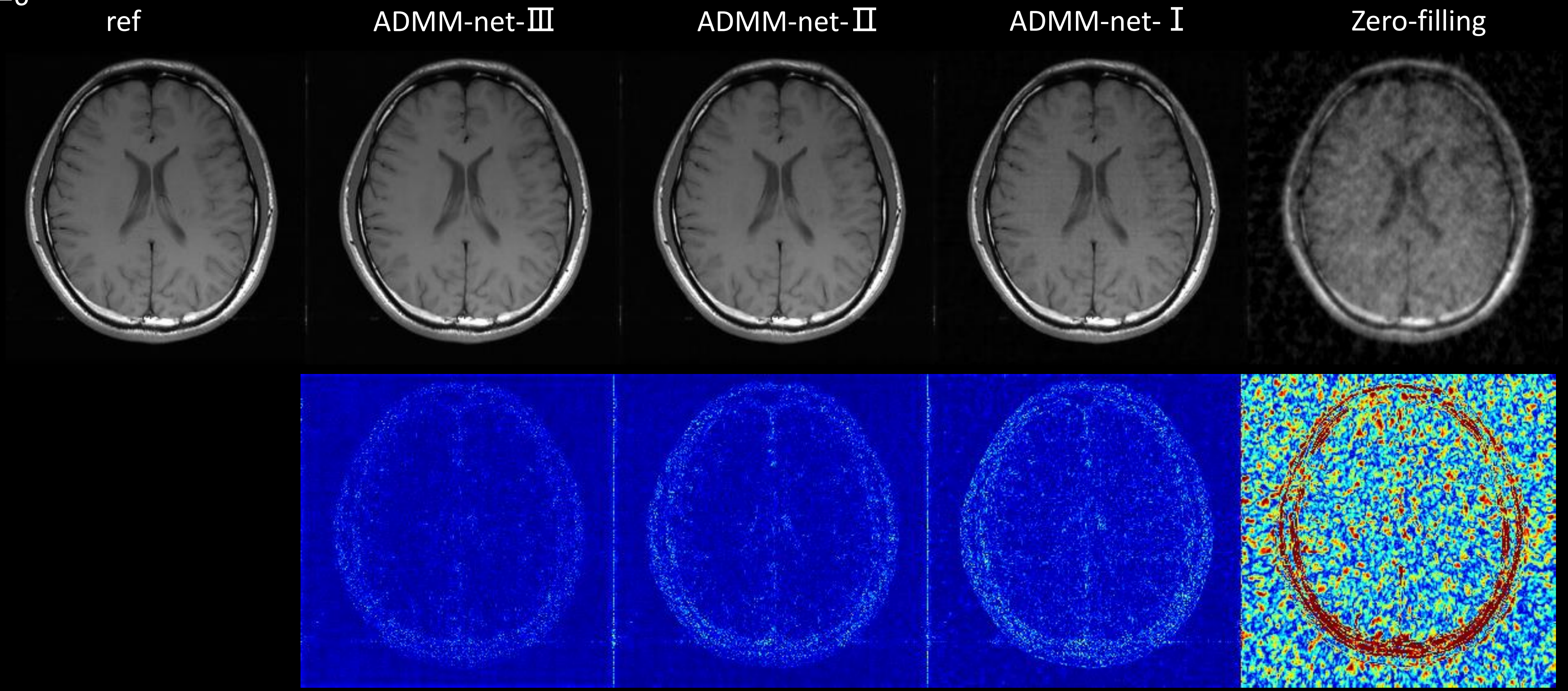

J Cheng and D Liang. http://arxiv.org/abs/1906.08143

PDHG-net

MR reconstruction

$$\min_m \frac{1}{2}\|Ax - f\|_2^2 + \lambda R(x)$$

Relaxing data consistency

MR reconstruction

$$\min_x \{F(Ax) + R(x)\}$$

Data fidelity (F(Ax)) **Regularization** (R(x))

Primal Dual Hybrid Gradient algorithm (Chambolle-Pock algorithm)

$$\begin{cases} d_{n+1} = \dfrac{d_n + \sigma(A\bar{x}_n - f)}{1+\sigma} \\ x_{n+1} = prox_\tau[R](x_n - \tau A^* d_{n+1}) \\ \bar{x}_{n+1} = x_{n+1} + \theta(x_{n+1} - x_n) \end{cases}$$

$$\begin{cases} d_{n+1} = prox_\sigma[F^*](d_n + \sigma A\bar{x}_n) \\ x_{n+1} = prox_\tau[R](x_n - \tau A^* d_{n+1}) \\ \bar{x}_{n+1} = x_{n+1} + \theta(x_{n+1} - x_n) \end{cases}$$

[1] J Alder et al. IEEE TMI2018 [2] J Cheng and D Liang. ISMRM2019 [3] J Cheng and D Liang. EMBC2019

PDHG-net

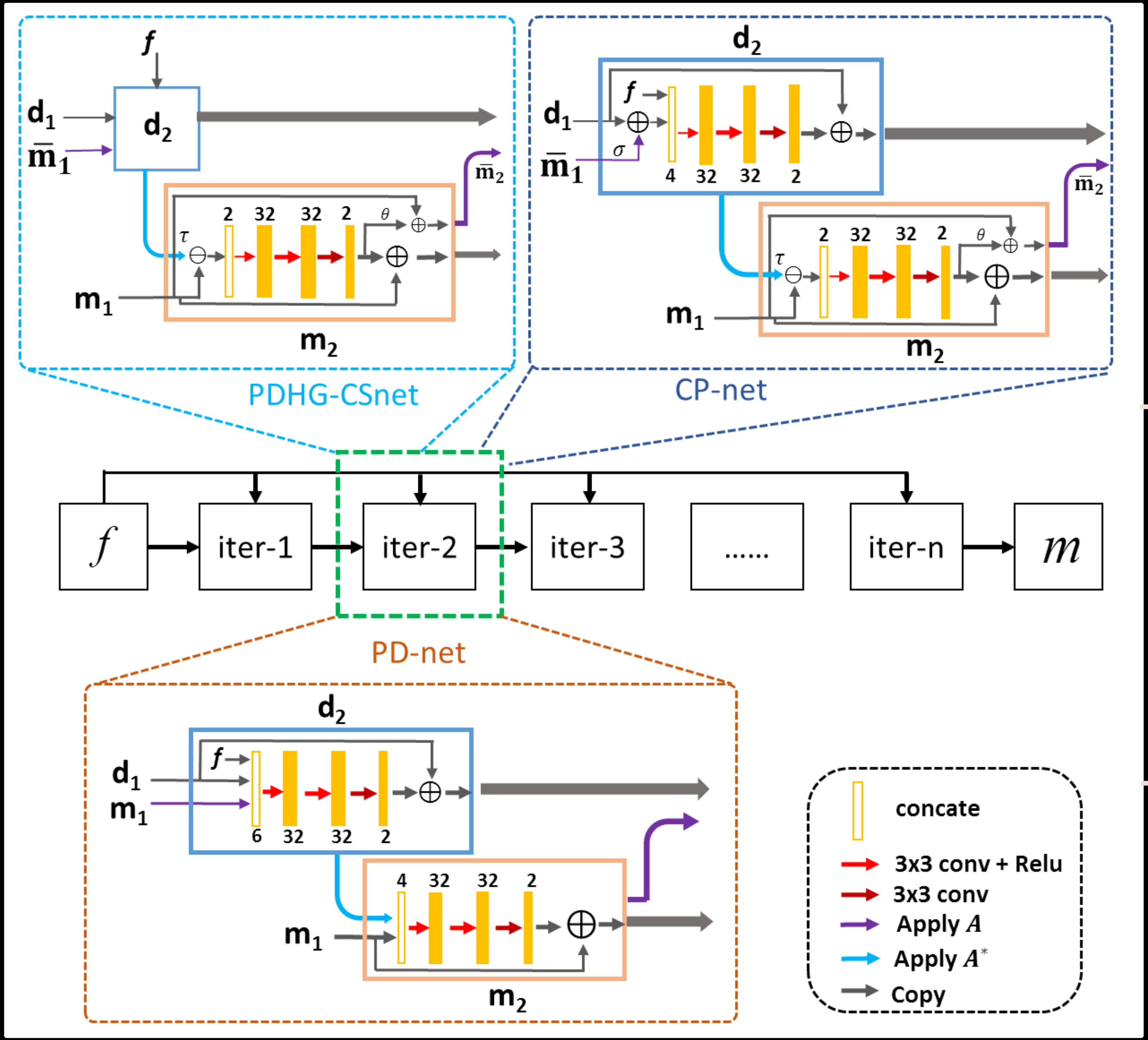

PDHG-net- Ⅰ

$$\|Ax - f\|_2^2 + \lambda R(x)$$

$$\begin{cases} d_{n+1} = \dfrac{d_n + \sigma(A\bar{x}_n - f)}{1+\sigma} \\ x_{n+1} = \Lambda(x_n - \tau A^* d_{n+1}) \\ \bar{x}_{n+1} = x_{n+1} + \theta(x_{n+1} - x_n) \end{cases}$$

PDHG-net- Ⅱ

$$d(Ax, f) + \lambda R(x)$$

$$\begin{cases} d_{n+1} = \Gamma(d_n + \sigma A\bar{x}_n, f) \\ x_{n+1} = \Lambda(x_n - \tau A^* d_{n+1}) \\ \bar{x}_{n+1} = x_{n+1} + \theta(x_{n+1} - x_n) \end{cases}$$

PDHG-net-Ⅲ

$$d(Ax, f) + \lambda R(x)$$

$$\begin{cases} d_{n+1} = \Gamma(d_n, Ax_n, f) \\ x_{n+1} = \Lambda(x_n, A^* d_{n+1}) \end{cases}$$

J Cheng and D Liang. MICCAI 2019

PDHG-net

R=4

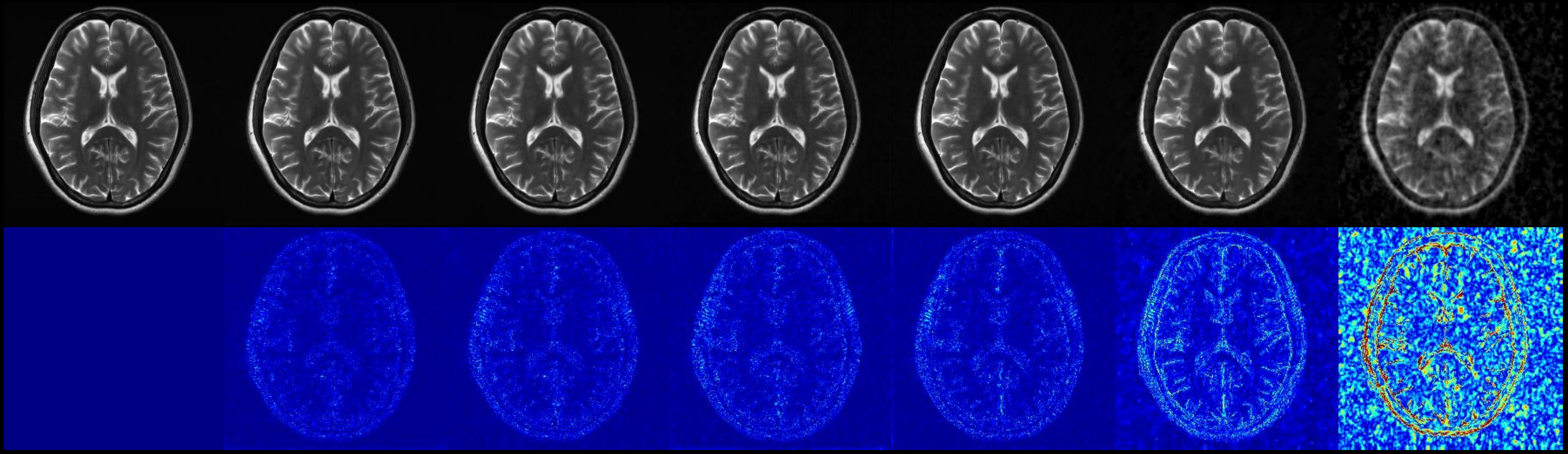

	reference	PDHG-net-Ⅲ	PDHG-net- Ⅱ	Basic-ADMM-CSNet	D5-C5	Rec_PF	Zero-filling
PSNR		**41.3688**	40.1125	38.9424	38.5734	34.1730	25.3383
SSIM		**0.9926**	0.9900	0.9874	0.9875	0.9396	0.6696

J Cheng and D Liang. MICCAI 2019   *J Cheng and D Liang. http://arxiv.org/abs/1906.08143*

ISTA-net

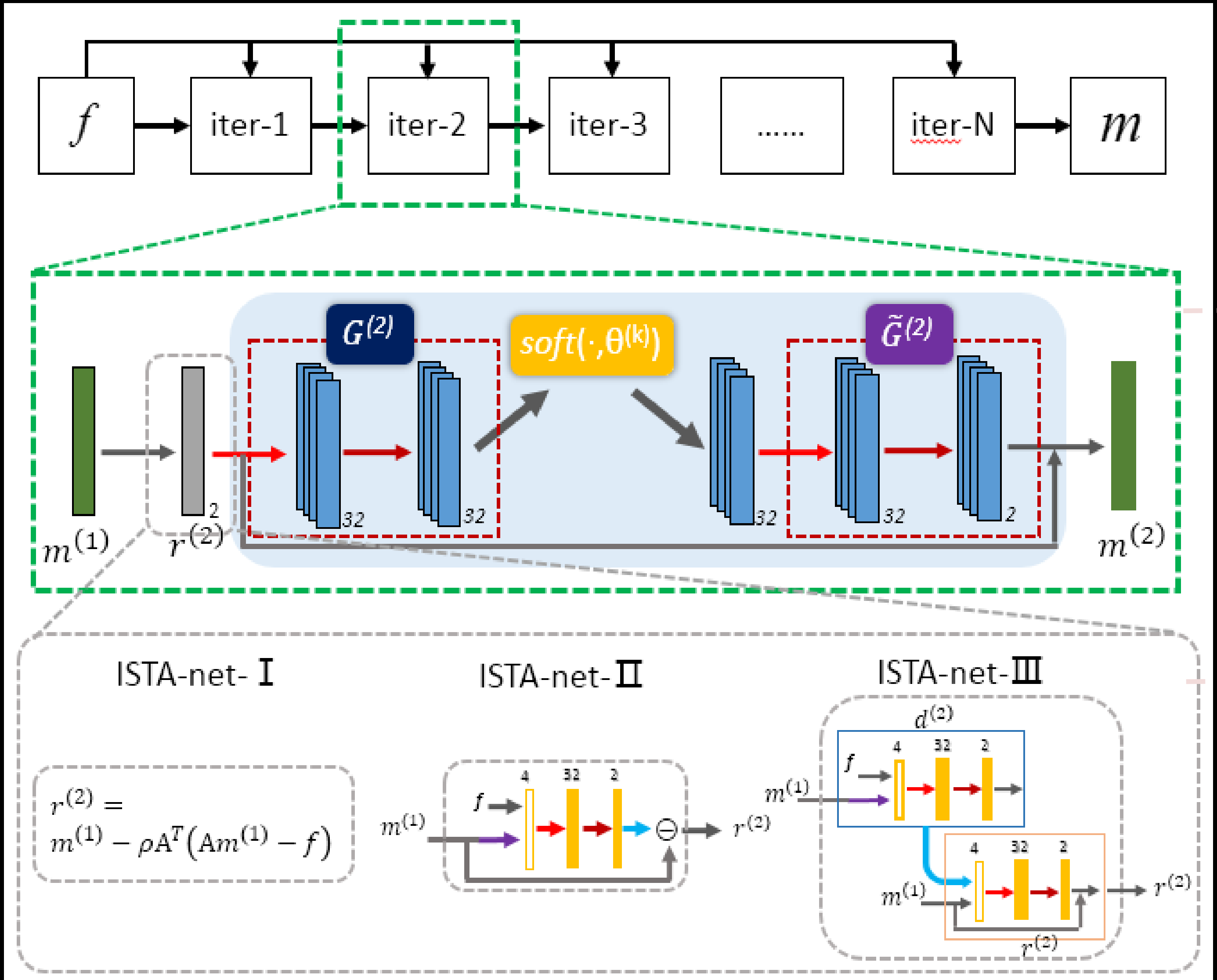

ISTA-net- I

$$\|Ax - f\|_2^2 + \lambda\|F(x)\|_1$$

$$\begin{cases} r^{(n+1)} = x^{(n)} - \rho A^T(Ax^{(n)} - f) \\ x^{(n+1)} = \tilde{F}(soft(F(r^{(n+1)}), \theta)) \end{cases}$$

ISTA-net- II

$$d(Ax, f) + \lambda\|F(x)\|_1$$

$$\begin{cases} d^{(n+1)} = \Gamma(Ax^{(n)}, f) \\ r^{(n+1)} = x^{(n)} - \rho A^T d^{(n+1)} \\ x^{(n+1)} = \tilde{F}(soft(F(r^{(n+1)}), \theta)) \end{cases}$$

ISTA-net-III

$$d(Ax, f) + \lambda\|F(x)\|_1$$

$$\begin{cases} d^{(n+1)} = \Gamma(Ax^{(n)}, f) \\ r^{(n+1)} = \Lambda(x^{(n)}, A^T d^{(n+1)}) \\ x^{(n+1)} = \tilde{F}(soft(F(r^{(n+1)}), \theta)) \end{cases}$$

J Zhang et al. CVPR2018 *J Cheng and D Liang. http://arxiv.org/abs/1906.08143*

Discussion: stability

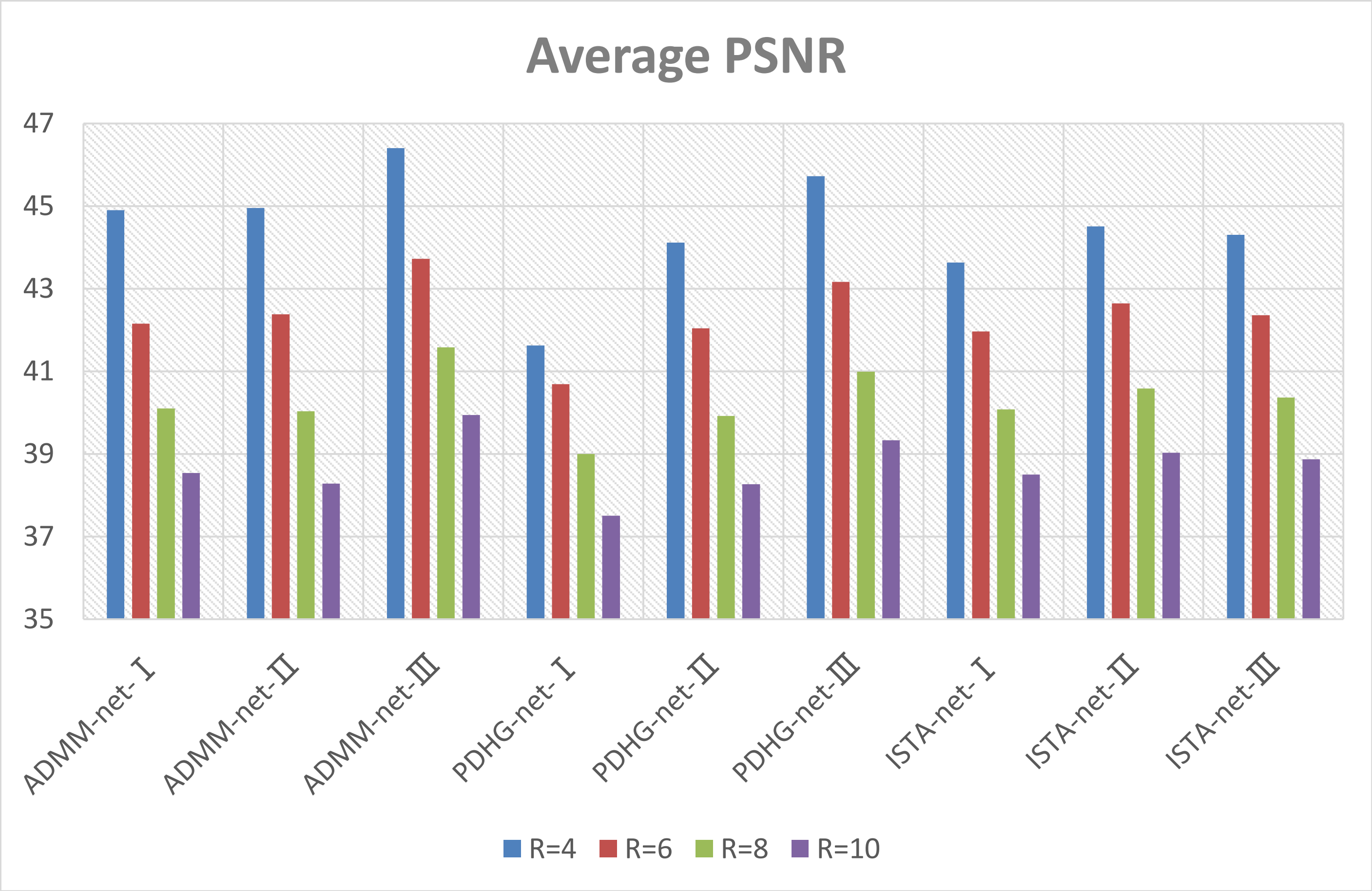

- Test data: 398 human brain 2D slices from 3D data
- 3D T1-weighted SPACE sequence, TE/TR=8.4/1000ms, FOV=$25.6\times25.6\times25.6cm^3$
- Poisson disk sampling
- Networks trained with R=6

More samples imply better reconstruction quality.

J Cheng and D Liang. http://arxiv.org/abs/1906.08143

Discussion: stability

R=6

error spectrum plots (ESP) with Fourier radial

ref

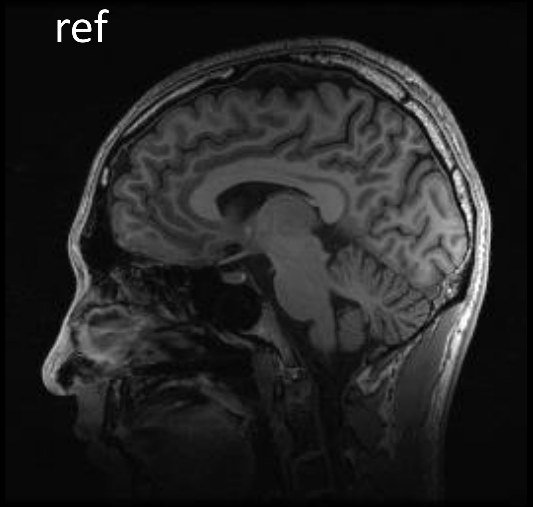

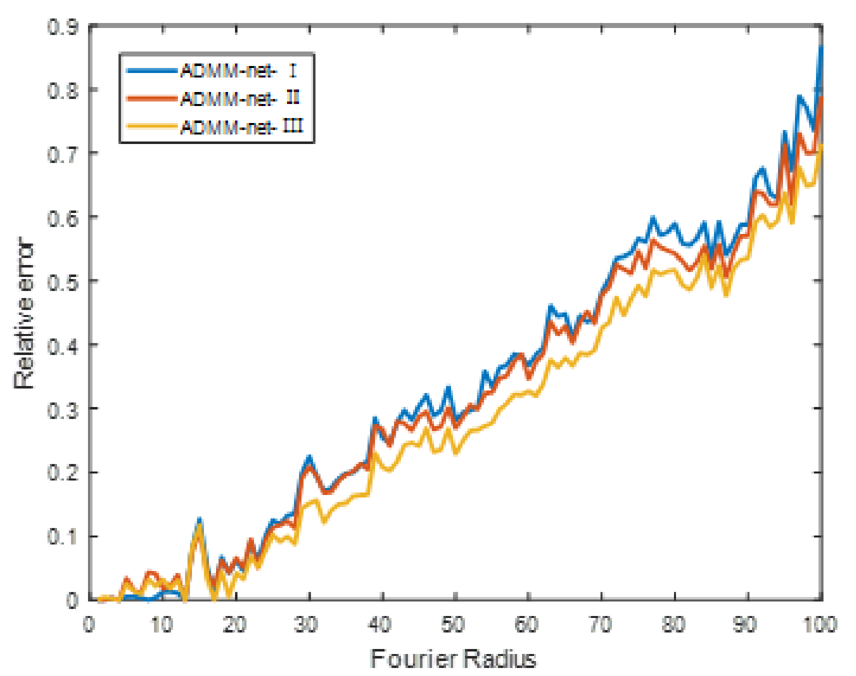

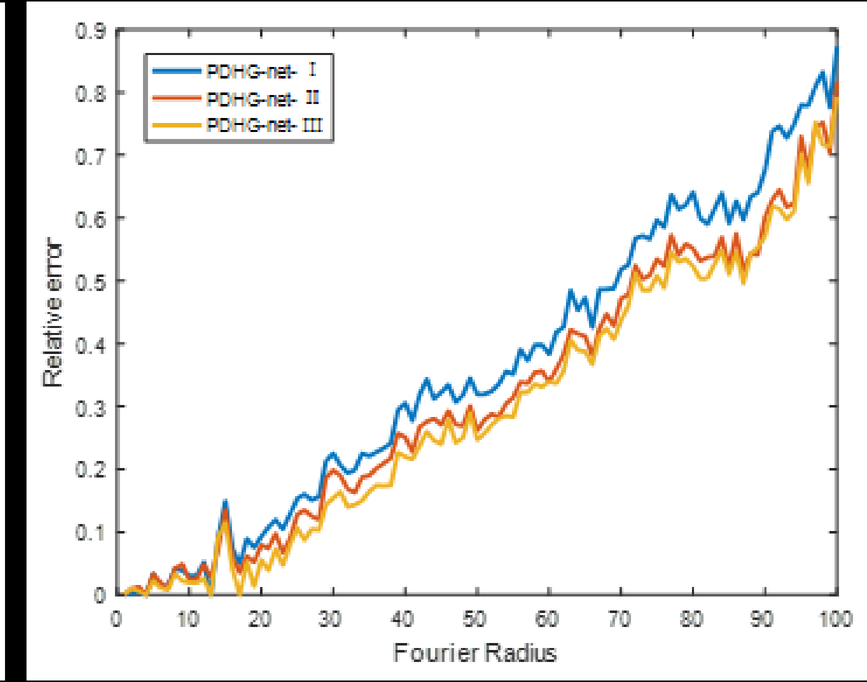

- ***the high frequency part of the image has higher error than low frequency part***
- ***state Ⅲ has the lowest***

J Cheng and D Liang. http://arxiv.org/abs/1906.08143

Discussion: stability

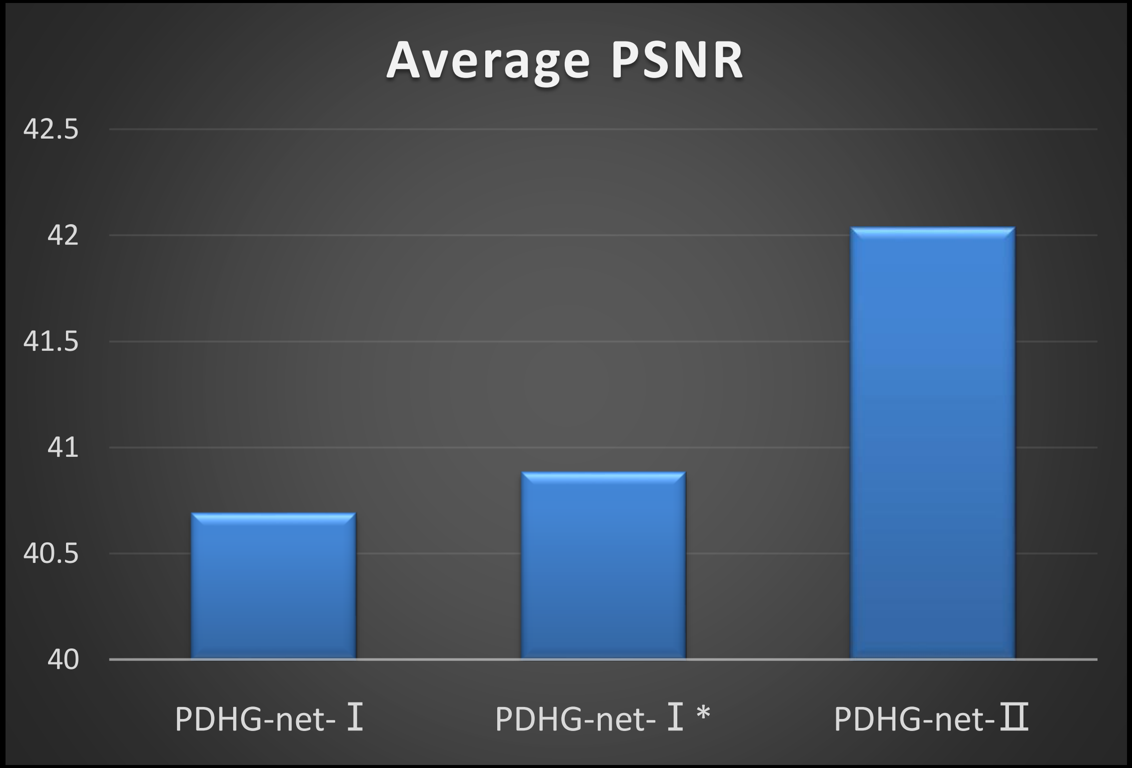

- R=6
- Test data: 398 human brain 2D slices from 3D data
- PDHG-net-Ⅱ has more parameters than PDHG-net- Ⅰ
- PDHG-net- Ⅰ * has the same structure as PDHG-net- Ⅰ but the same number of parameters as PDHG-net-Ⅱ

the improvement from state Ⅰ to state Ⅱ is induced by the learned data fidelity rather than the deeper network.

J Cheng and D Liang. unpublished data

ADMM-Net-III Test in Industry

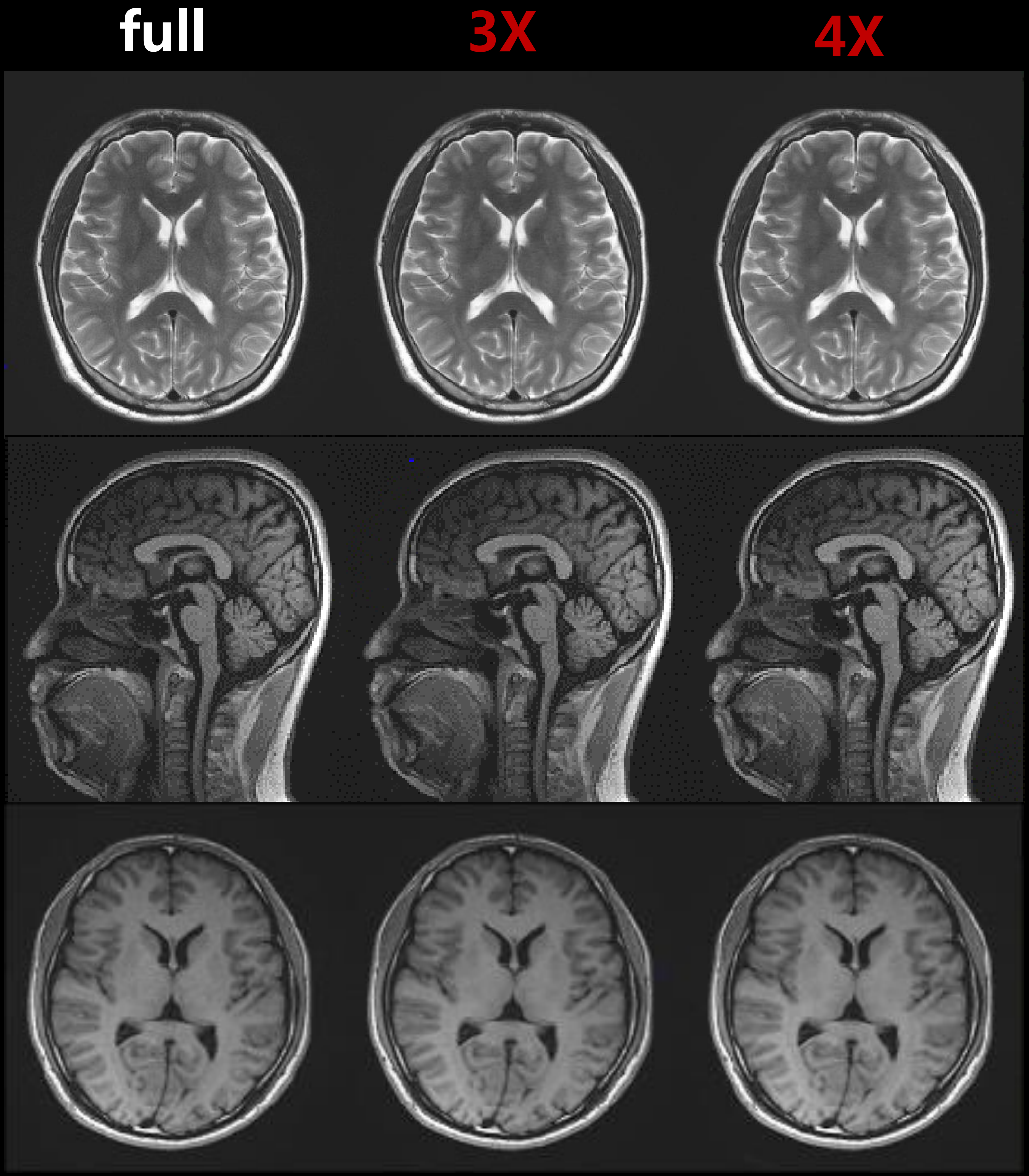

ADMM-Net-III Test in Industry

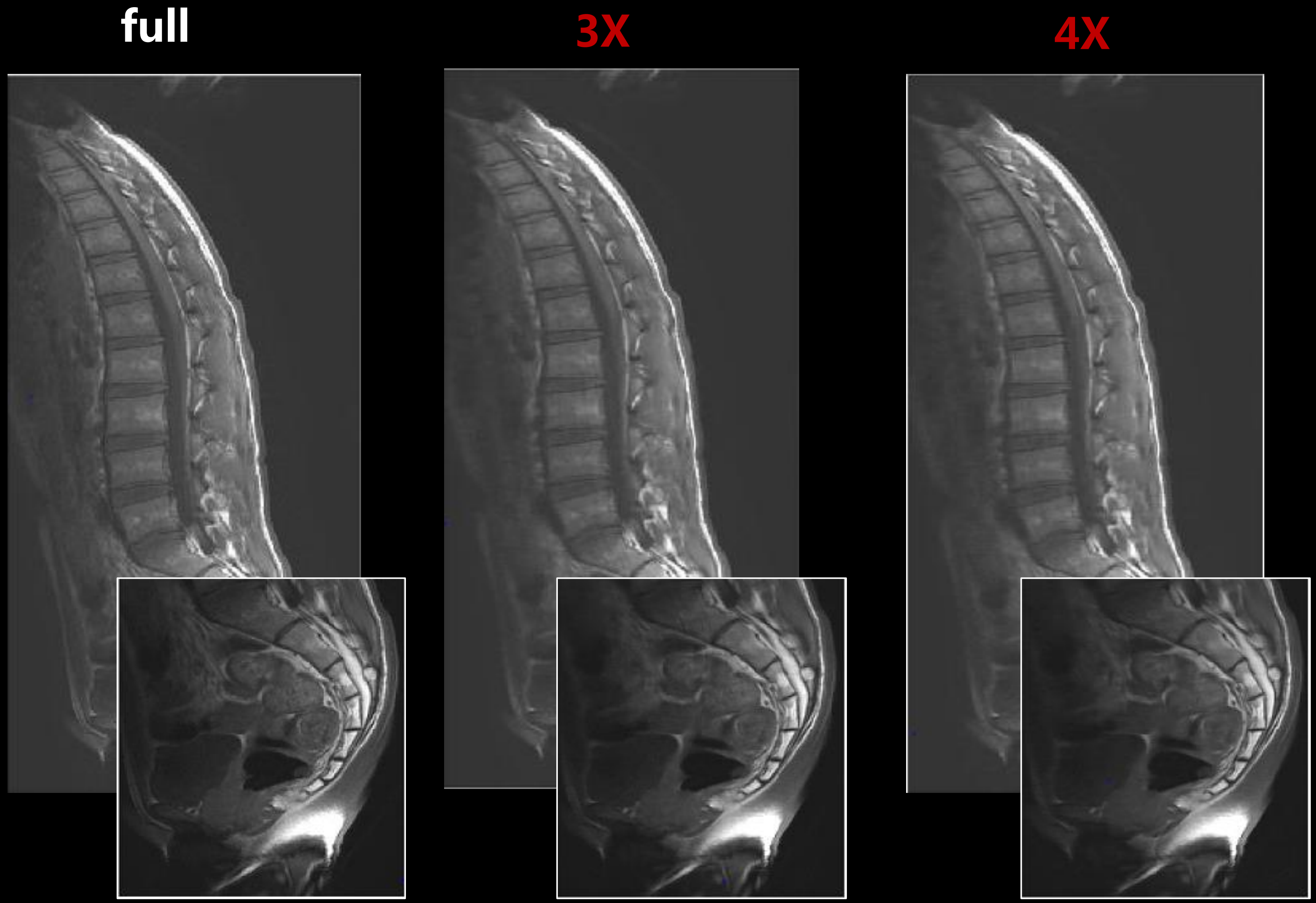

ADMM-Net-III MR VWI in Industry

Left
MCA 2

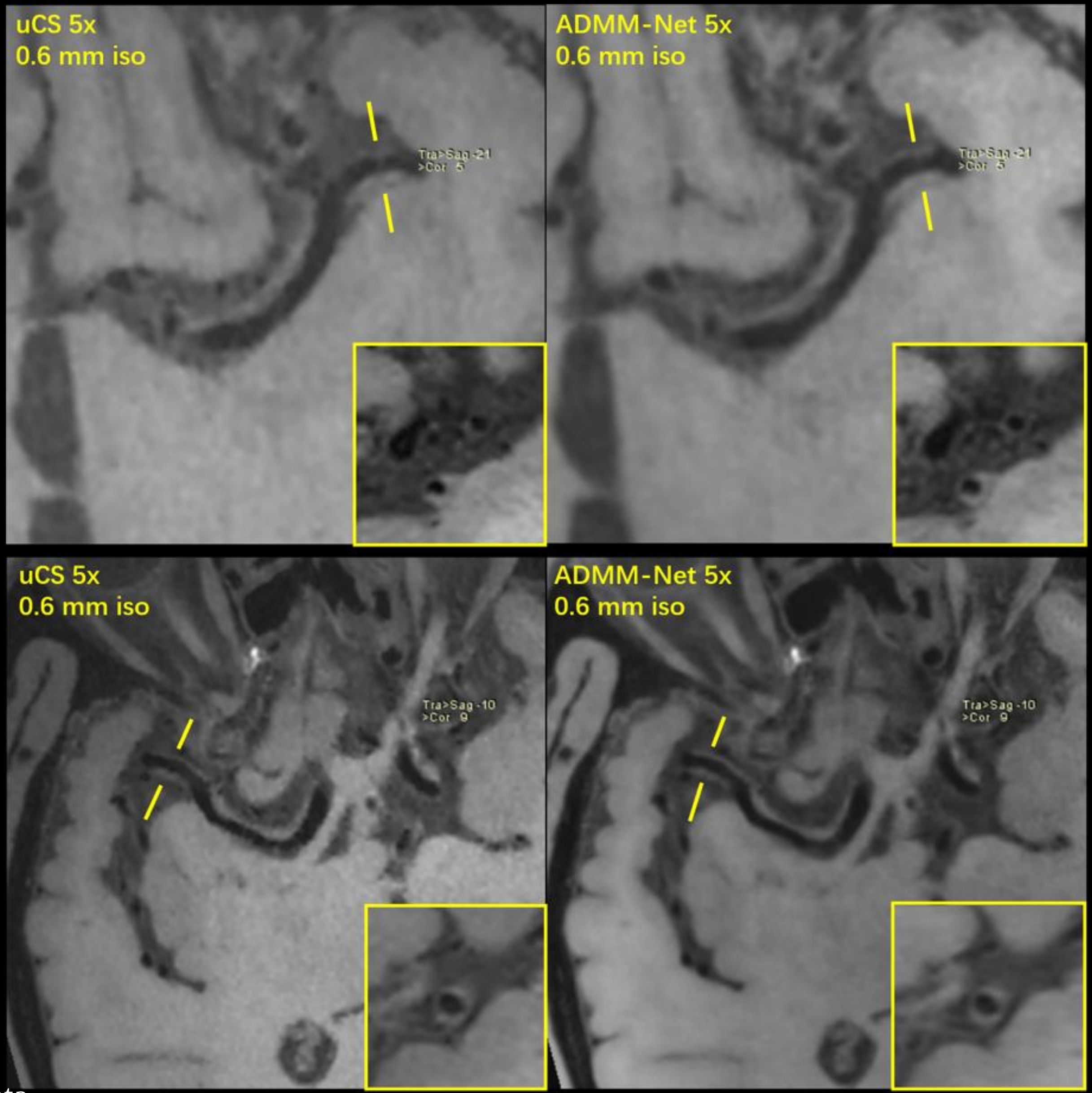

Right
MCA 2

62 years old
Male
TA = 4:48

The ADMM-Net-III gave better SNR and wall depiction quality.

S Jia and J Cheng
et al. unpublished data

ADMM-Net-III MR VWI in Industry

basilar artery

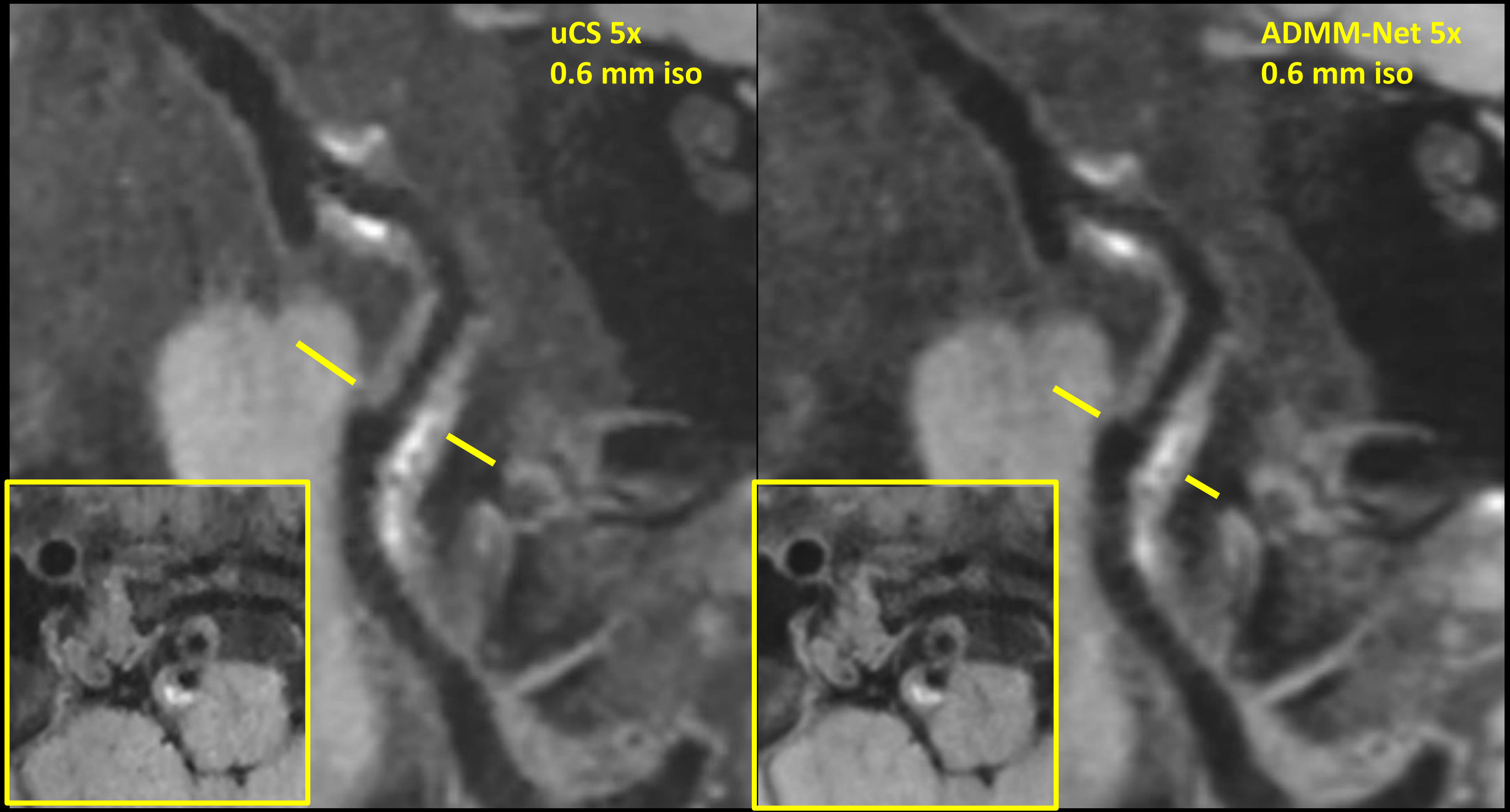

The ADMM-Net-III gave slightly better SNR and similar wall depiction quality.

S Jia and J Cheng et al. unpublished data

Deep Learning MRI: a big picture

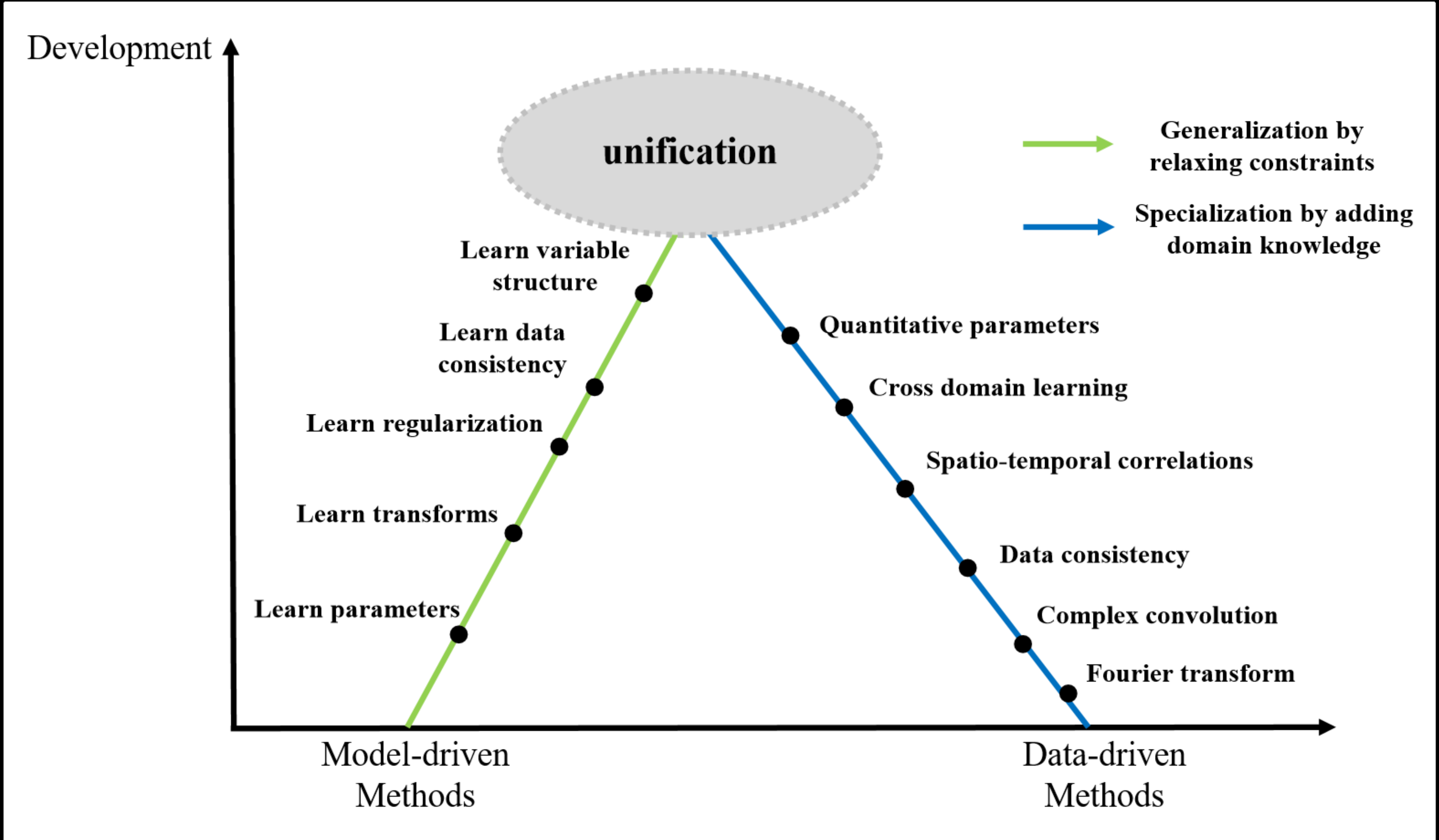

[1] Y. Yang et al, IEEE PAMI 2018.[2]K. Hammernik, et al, MRM 2018. [3]J. Zhang et al, CVPR 2018. [4]H. K. Aggarwal et al, IEEE TMI 2019. [5]J. Schlemper, et al, IEEE TMI 2018. [6] J. Adler et al, IEEE TMI 2018. [7]J. Cheng et al, MICCAI 2019. [8]C. Qin et al, IEEE TMI 2019. [9]S. Wang et al, ISBI 2016. [10]K. Kwon et al, Med Phys 2017. [11]B. Zhu et al, Nature 2018. [12]T. M. Quan et al, IEEE TMI 2018. [13]M. Mardani et al, IEEE TMI 2019. [14]Y. Han et al, MRM 2018. [15]M. Akcakaya et al, MRM 2019. [16]D. W. Lee et al, IEEE TBME 2018. [17]A. Hauptmann et al, MRM 2019. [18]S. Wang et al, NMR in Biomedicine 2019. [19]T. Eo et al, MRM 2018. [20]C. Cai et al, MRM 2018. [21]F. Liu et al, MRM 2019. [22]J. Yoon et al, Neuroimage 2018. [23]O. CohenMRM 2018.

Roadmap of medical imaging equipment

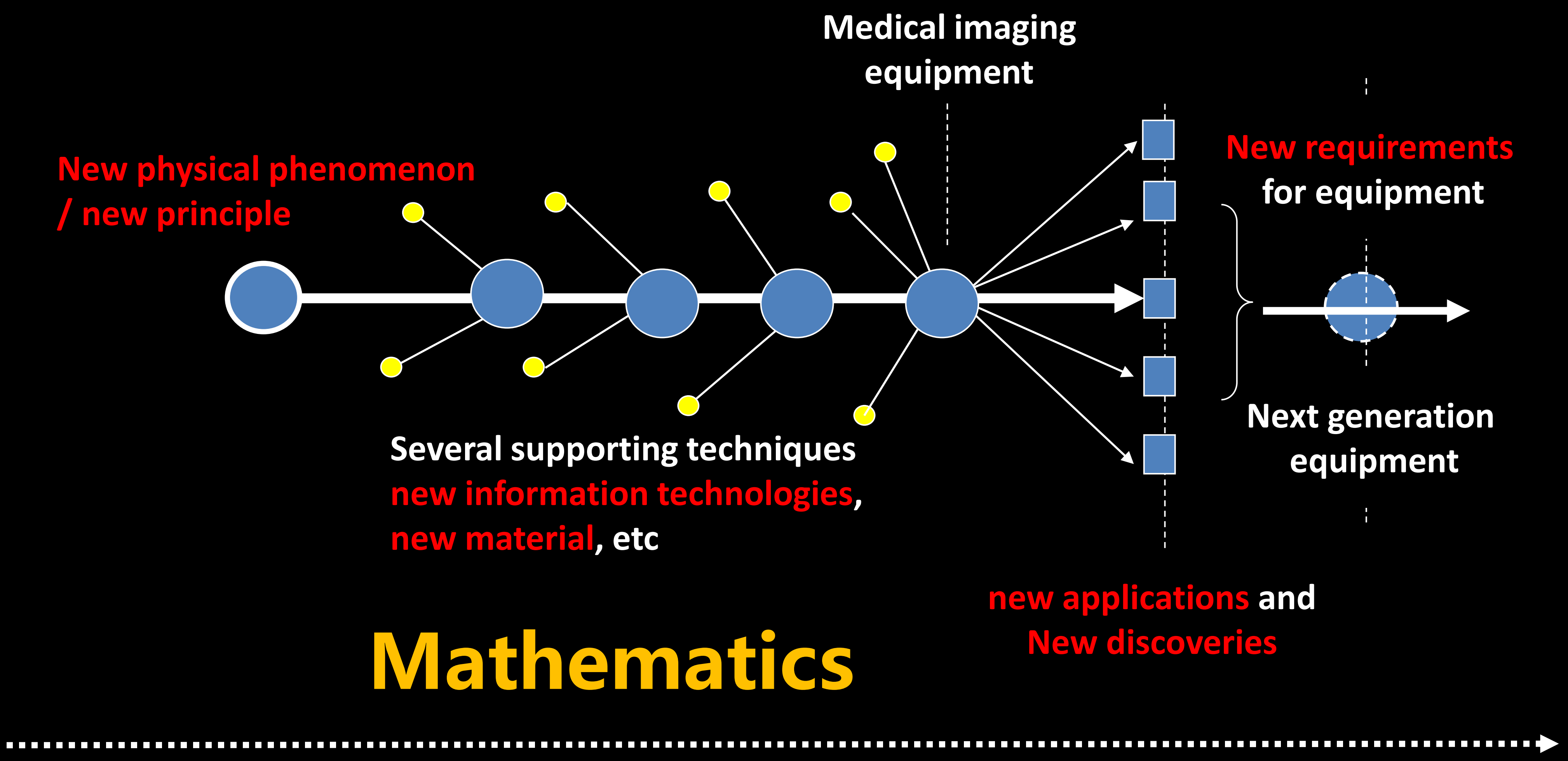

Acknowledgement

- **Collaborators:**
  - Leslie Ying(UB)
  - Yuchou Chang(Houston)
  - Qiegen Liu(NCU)
  - Yio-Chu Chung (Siemens)
- **My colleges and students at SIAT:**
  - YanJie Zhu
  - Haifeng Wang
  - Shanshan Wang
  - Lei Zhang
  - Sen Jia
  - Jing Cheng
  - Ziwen Ke
- **Funding support**
  - National Science Foundation of China
  - Chinese Academy of Sciences
  - Shenzhen Basic Research Program

Thanks!